

Adaptive encodings for small and fast compressed suffix arrays

DIEGO DÍAZ-DOMÍNGUEZ and VELI MÄKINEN, Department of Computer Science, University of Helsinki, Finland

Compressed suffix arrays index large repetitive collections and are widely used in bioinformatics, version control, and natural language processing. The r -index and its variants combine the run-length Burrows–Wheeler transform (BWT) with a sample of the suffix array to achieve space proportional to the number of equal-symbol runs. While effective for near-identical strings, their size grows quickly when edited copies are added to the collection as the number of BWT runs is sensitive to variation. Existing approaches either apply extra compression at the cost of slower queries or prioritize speed at the expense of space, limiting practical tradeoffs at large scale.

We introduce *variable-length blocking* (VLB), an adaptive encoding for BWT-based compressed suffix arrays. Our technique adapts the amount of indexing information to the local run structure: compressible regions retain less auxiliary data, while incompressible areas store more. Specifically, we recursively partition the BWT until each block contains at most w runs (a parameter), and organize the blocks into a tree. Accessing a position requires descending a root-to-leaf path followed by a short run scan. Compressible regions are placed near the root, while incompressible regions lie deeper and are augmented with additional indexing data to speed up access. This strategy balances space and query speed by reallocating bits saved in compressible areas to accelerate access to incompressible ones. The VLB-tree also improves memory locality by colocating related BWT and suffix array information.

Backward search relies on rank and successor queries over the BWT. We introduce a sampling technique that relaxes global correctness by guaranteeing that these queries are correct only along valid backward-search states. This restriction reduces space usage without affecting the speed or correctness of pattern matching.

We further extend the concepts of the VLB-tree to encode suffix array samples and then to the subsampled r -index (sr -index), thus producing a small fully-functional compressed suffix array. Experiments show that VLB-tree variants outperform the r -index and sr -index in query time, while retaining space close to that of the sr -index. The move data structure, a recent encoding, achieves better speed performance than the VLB-tree but uses considerably more space, yielding a clear space–time tradeoff.

CCS Concepts: • Theory of computation → Data compression; Pattern matching; • Applied computing → Computational genomics.

Additional Key Words and Phrases: Burrows–Wheeler Transform, compressed suffix arrays, pattern matching, adaptive encoding, large and repetitive collections

ACM Reference Format:

Diego Díaz-Domínguez and Veli Mäkinen. 2026. Adaptive encodings for small and fast compressed suffix arrays. *ACM Trans. Algor.* 1, 1 (February 2026), 28 pages. <https://doi.org/10.1145/nnnnnnnn.nnnnnnnn>

1 Introduction

The search for patterns in large collections of strings is a fundamental task in information retrieval, data mining, and bioinformatics. This problem has been studied for decades, producing iconic solutions such as the suffix array [22] or

Authors' Contact Information: [Diego Diaz-Domínguez](#), diego.diaz@helsinki.fi; [Veli Mäkinen](#), veli.makinen@helsinki.fi, Department of Computer Science, University of Helsinki, Helsinki, Uusimaa, Finland.

Permission to make digital or hard copies of all or part of this work for personal or classroom use is granted without fee provided that copies are not made or distributed for profit or commercial advantage and that copies bear this notice and the full citation on the first page. Copyrights for components of this work owned by others than the author(s) must be honored. Abstracting with credit is permitted. To copy otherwise, or republish, to post on servers or to redistribute to lists, requires prior specific permission and/or a fee. Request permissions from permissions@acm.org.

© 2018 Copyright held by the owner/author(s). Publication rights licensed to ACM.

Manuscript submitted to ACM

the suffix tree [29], but our ability to accumulate textual data has far exceeded the limits of those solutions, motivating the development of compressed indexes. Large collections are often repetitive, and these repetitions induce regularities in suffix arrays and trees that the compressed variants exploit to reduce space. However, the continuous accumulation of data and the development of new technologies have led to the creation of even larger collections that can reach the terabyte scale, and even compressed solutions fall short in this context.

Compressed suffix arrays are space-efficient indexes that support the same two basic queries as plain suffix arrays: *count* and *locate* the occurrences of a pattern in a text. Several variants have been proposed [12, 16, 26], with the FM index [11] being the most widely used. The FM index represents a string $S[1..n]$ via the Burrows–Wheeler transform (BWT) [5] plus a sample of the suffix array $SA[1..n]$ of S , and fits in $nH_k(S) + o(n \log \sigma)$ bits, where H_k is the k -th order entropy of S and σ is the alphabet size. Given a pattern $P[1..m]$, it reports the occ matches in $O(m \log \sigma + occ \log^{1+\epsilon} n)$ time for any constant $\epsilon > 0$. In practice, its space is close to $n \log \sigma$ bits, far below the $n(\log \sigma + \log n)$ bits needed to support *count* and *locate* with S and the plain suffix array. This efficiency has made the FM index a workhorse in genomics [18, 20], yet even space close to the plain-text representation can be prohibitive at massive scales.

The r -index of Gagie et al. [12] is a variant of the FM index that reduces the space to $O(r)$ by run-length encoding the BWT and sampling $2r$ elements of the SA, where r is the number of equal-symbol runs in the BWT. In collections of near-identical sequences, r is much smaller than n , achieving important space reductions that have motivated new r -index-based data structures [1, 4, 7, 10, 25, 27, 30] for genomic analysis. However, the BWT is sensitive to edits, as a single text modification can increase r by a $\Theta(\log n)$ factor [13]. The sensitivity rapidly increases r with new variation until the r -index approaches the size of the FM index [6]. This poses a problem for terabyte-scale collections, where the level of repetitiveness is often not extreme.

An important observation is that runs are distributed unevenly, with some BWT areas having few long runs, while others have many short runs; the suffix array samples of the r -index show a similar locality. This property makes uniform encoding inefficient and motivates adaptive schemes. Existing approaches only partially exploit this idea: the fixed block boost of Gog et al. [15] breaks the BWT into equal-length blocks and encodes them independently, while the *subsampled r*-index (or *sr*-index) of Cobas et al. [6] discard values of *SA* from text areas where the sampling is dense. These techniques help but remain coarse or limited in scope.

Another challenge is query speed, as searching for long patterns in BWT-based indexes triggers multiple cache misses. The move data structure of Nishimoto and Tabei [23] alleviates this problem by reorganizing the run-length BWT data in a cache-friendly manner, achieving significantly faster queries than the r -index but at the cost of being 2-2.5 times larger [2, 9]. Thus, existing work splits into two directions: minimizing space (*sr*-index) or maximizing speed (*move*), with no structure achieving both.

Our contribution. We present *variable-length blocking* (VLB), a technique for representing BWT-based compressed suffix arrays that balances query speed and space usage. We exploit the skewed distribution of BWT runs to redistribute indexing costs. We recursively divide the BWT into variable-length blocks so that each block contains a bounded number of runs, and organize the output in a hierarchical structure (the VLB-tree). Compressible blocks remain near the root and require little auxiliary data, while less compressible regions induce deeper subtrees enriched with additional indexing information. This non-uniform layout reallocates space from areas where access is fast to areas where queries are more expensive, yielding a structure whose depth and space adapts to the compressibility of the BWT.

- The VLB-tree (Section 3): we formalize the VLB-tree and analyze its performance. Given a block size ℓ , branching factor f , and run threshold w , a query traverses a tree path of height $O(\log_f(\ell/w))$ and scans at most w

consecutive runs in a leaf. Counting the occurrences of a pattern $P[1..m]$ takes $O(m(\log_f(\ell/w) + w))$ time. Importantly, processing each query symbol incurs approximately one cache miss in sparse BWT regions and up to $\log_f(\ell/w)$ cache misses in dense, high-run regions, assuming w consecutive runs fit the cache.

- Counting with toehold (Section 4): we integrate suffix array samples within the VLB-tree so that an occurrence of the pattern can be extracted cache-efficiently while counting. Similarly to the r -index, this occurrence serves as a toehold to decode the other text positions.
- VLB-tree sampling (Section 5): we introduce a sampling mechanism for rank and successor queries; core operations for pattern matching. The sampled data relax global correctness, only guaranteeing correct answers when the output induces a BWT range that is reachable during pattern matching. By exploiting the invariants of backward search, we reduce index space without affecting the pattern-matching speed or correctness. This relaxation principle is independent of VLB and may be applicable to other indexing schemes.
- VLB-tree for ϕ^{-1} (Section 6): we extend the VLB-tree to represent the ϕ^{-1} function, which decodes the occurrences of a pattern from its toehold. The combined VLB-trees of the BWT and ϕ^{-1} yield a compressed suffix array equivalent to the r -index. Section 7 describes how to subsample this representation to produce a cache-friendly sr -index, including a fast variant that speeds up the location of pattern occurrences.

We implemented two VLB-based data structures: a run-length BWT supporting *count* queries and a fast *sr*-index supporting both *count* and *locate*. Our experiments show speedups of up to 5.5 for *count* queries and 9.77 for *locate* queries over state-of-the-art alternatives. In terms of space, our run-length BWT achieves up to a 2-fold reduction, while our *sr*-index requires space comparable to that of Cobas et al. [6]. Although the move data structure [2, 23] attains faster query times, it does so at the cost of being typically 2.55–8.33 times larger, yielding a less favorable space–time tradeoff. Finally, cache-miss measurements indicate that the performance gains of our framework are largely due to its cache-aware hierarchical layout, underscoring its practical impact.

2 Preliminaries

Strings. A string $S[1..n]$ is a sequence of n symbols over an alphabet $\Sigma = \{1, 2, \dots, \sigma\}$, where the smallest symbol is a sentinel $1 = \$$ that appears only at the end ($S[n] = \$$). A *run* is a maximal equal-symbol substring $S[h..t] = c^{t-h+1}$, with *head* $S[h]$ and *tail* $S[t]$. The run-length encoding of $S[1..n] = c_1^{l_1} c_2^{l_2} \dots c_r^{l_r}$ is *rle*(S) = $(c_1, l_1)(c_2, l_2) \dots (c_r, l_r)$.

Operations over sequences. For $c \in \Sigma$, $rank_c(S, i)$ is the number of occurrences of c in $S[1..i]$, and $select_c(S, j)$ is the position of the j -th occurrence of c in S . The queries $succ_c(S, j)$ and $pred_c(S, j)$ return the nearest occurrence of c at or after j , and at or before j , respectively (returning $n + 1$ and 0 if no such occurrence exists).

2.1 The suffix array

The *suffix array* $SA[1..n]$ [22] is a permutation of $[1..n]$ that lists the suffixes of S in increasing lexicographic order. Its inverse $ISA[1..n]$ stores positions such that $ISA[j] = i$ iff $SA[i] = j$. The *SA* supports two fundamental queries. The operation $count(P[1..m])$ returns the number of occurrences of $P \in \Sigma^*$ in S , and $locate(P[1..m])$ returns the set $O \subset [n]$ of indices such that for each $i \in O$, $S[i..i+m-1] = P[1..m]$.

A concept related to the suffix array is the ϕ^{-1} function:

Definition 2.1. (Definition 2 [12]) Let i be a text position and let $ISA[i] = j$ be the corresponding index for $SA[j] = i$. The function ϕ^{-1} is a permutation of $[1..n]$ defined as

$$\phi^{-1}(i) = \begin{cases} SA[j+1] = SA[ISA[i]+1] & \text{if } j < n \\ SA[1] = n & \text{if } j = n. \end{cases}$$

2.2 The Burrows–Wheeler transform

The Burrows–Wheeler transform (BWT) [5] of S is a reversible permutation $BWT(S) = L[1..n]$ that enables compression and fast pattern search. It is defined as $L[j] = S[SA[j]-1]$ when $SA[j] \neq 1$, and $L[j] = \$$ when $SA[j] = 1$.

Let $F[1..n]$ be the first column of the suffixes of S sorted in lexicographic order, and let $C[1..\sigma]$ be an array storing in $C[c]$ the number of symbols in F that are smaller than c . The LF mapping $LF(j) = C[L[j]] + rank_{L[j]}(L, j)$ links $L[j]$ to $F[LF(j)] = F[ISA[SA[j]-1]]$. Moreover, visiting the $k+1$ positions $L[j], L[LF(j) = j_2], L[LF(j_2) = j_3], \dots, L[LF(j_k) = j_{k+1}]$ spells $S[SA[j]-1-k..SA[j]-1]$ from right to left. Applying LF mapping k times from $L[j]$ is commonly denoted $LF^k(j) = j_{k+1}$.

Backward search. The query $backwardsearch(P) = (sp_1, ep_1)$ returns the range $SA[sp_1..ep_1]$ of suffixes in S prefixed by $P[1..m]$, where $ep_1 - sp_1 + 1 = count(P)$. In each step $l \in \{m+1, m, \dots, 2\}$, the algorithm obtains the range $SA[sp_{l-1}..ep_{l-1}]$ of suffixes in S prefixed by $P[l-1..m]$ using the formula

$$\begin{aligned} sp_{l-1} &= C[P[l-1]] + rank_{P[l-1]}(L, sp_l - 1) + 1 \\ ep_{l-1} &= C[P[l-1]] + rank_{P[l-1]}(L, ep_l). \end{aligned} \tag{1}$$

The process starts with $sp_{m+1} = 1$ and $ep_{m+1} = n$, which represents the empty string $P[m+1..m]$, and iteratively refines the range $SA[sp_{l-1}..ep_{l-1}]$ until it reaches $SA[sp_1..ep_1]$ after m steps.

2.3 BWT-based compressed suffix arrays

A compressed suffix array encodes L with support for queries *backwardsearch* and *LF* together with a sample of suffix array values. A *locate*(P) query runs *backwardsearch*(P) = (sp_1, ep_1) and recovers the non-sampled elements of $SA[sp_1..ep_1]$ using the links between L , S , and SA . Representative designs include the FM-index [11], the *r*-index [12], and the subsampled *r*-index [6].

2.3.1 The *r*-index. This data structure samples two elements of SA per BWT run and stores L in a run-length encoded format that supports *LF* mapping and backward search. The suffix array samples are encoded as follows:

- An array $SA_h[1..r]$ stores in $SA_h[u]$ the value $SA[h_u]$ associated with the u -th run $L[h_u..t_u]$.
- A bitvector $B[1..n]$ marks each position $B[SA[t_u]] = 1$ associated with the tail t_u of $L[h_u..t_u]$.
- An array $D[1..r]$ stores in $D[rank_1(B[SA[t_u]])]$ the difference $SA[h_{u+1}] - SA[t_u]$ between the head and tail of consecutive runs.

Figure 1 shows an example of these components.

The *r*-index answers the query *locate*(P) using a modified¹ version of *backwardsearch*(P) = $(sp_1, ep_1, SA[sp_1])$ that returns the first value $SA[sp_1]$, and later uses $SA[sp_1]$ as a *toehold* to locate the elements of $SA[sp_1 + 1..ep_1]$ with ϕ^{-1} .

Counting with toehold. As *backwardsearch*(P) visits the ranges $(sp_{m+1}, ep_{m+1}), (sp_m, ep_m), \dots, (sp_2, ep_2)$, it maintains the index sp_g for the smallest step g with $L[sp_g] \neq P[g-1]$, initially setting $sp_g = 1$ and $g = m+1$. Once the

¹We note that the *r*-index is often described in the literature right to left: storing run tails and using the inverse of ϕ^{-1} . However, we defined left to right for compatibility with our method.

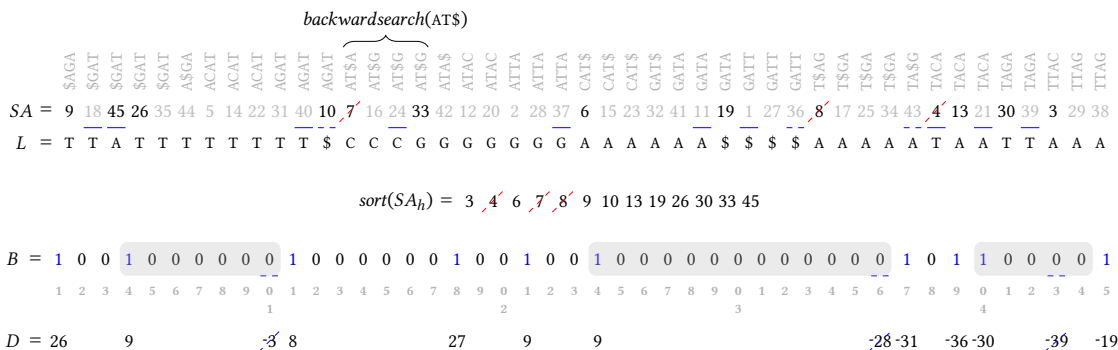


Fig. 1. Components of the r -index and sr -index ($s = 3$) for $S = \text{GATTACAT\$AGATACAT\$GATACAT\$GATTAGAT\$GATTAGATA\$}$. Vertical strings are the partial suffixes of S in lexicographical order. The black values in SA correspond to the sample SA_h . Values of SA underlined in blue are the marked positions in B . The canceled values in SA were originally in SA_h but they were discarded after subsampling. The dashed underlined values in SA are the positions in B that are cleared because of subsampling. Each gray region in B is a partially valid area, with the underlined 0 (cleared) marking the start of the invalid suffix. In D , canceled values are discarded because their bits in B were cleared.

algorithm obtains (sp_1, ep_1) , it finds the index ρ of the leftmost run $L[h_\rho..t_\rho]$ within $L[sp_g..ep_g]$ with $L[h_\rho] = P[g - 1]$. This information is enough to compute the toehold

$$SA[sp_1] = SA_h[\rho] - (m - g + 2). \quad (2)$$

To retrieve ρ , the r -index uses a special successor query, say $rsucc$, that returns the index of the BWT run where the successor lies, which in this context translates to $rsucc_{P[g-1]}(L, sp_g) = \rho$.

Locating from toehold. The r -index obtains $SA[sp_1 \dots ep_1]$ iteratively by performing $\phi^{-1}(SA[j]) = SA[j + 1]$ from $j = sp_1$. The difference $d = SA[j + 1] - SA[j]$ between values $SA[j]$ and $SA[j + 1]$ that fall within the same run $L[h_u \dots t_u]$, with $h_u \leq j < t_u$, is invariant under LF operations as long as the traversal remains within the same run. Consequently, the difference between suffix array values changes only when crossing a run boundary.

This property allows the r -index to encode ϕ^{-1} using a single difference per run. Let b be the largest index such that $B[b] = 1$ and $b \leq SA[i]$. Then,

$$\phi^{-1}(SA[j]) = SA[j] + D[rank_1(B, SA[j])] = SA[j + 1]. \quad (3)$$

Thus, ϕ^{-1} reduces to a predecessor query on B followed by a lookup in D .

2.3.2 *The subsampled r-index.* The *sr*-index reduces space by discarding suffix array samples in dense regions of SA_h . Removed samples invalidate some regions of the index, which are reconstructed at query time via *LF* operations. This approach significantly reduces space while preserving good query performance.

Let $p_1 < p_2 < \dots < p_r$ be the sorted values of SA_h , and let $s < n$ be a sampling parameter. For any $1 < a < r$, the sample p_a is discarded from SA_h if $p_{a+1} - p_{a-1} \leq s$. The test is applied sequentially for $a = 2, 3, \dots, r - 1$. Thus, if p_a is removed, the next step checks if $p_{a+2} - p_{a-1} \leq s$ to decide whether p_{a+1} is sampled, applying the same procedure to the remaining elements of SA_h .

A bitvector $R[1..r]$ now marks the runs in L that were subsampled. A rank structure maps the retained samples to their positions in the reduced array SA_h . Moreover, for each discarded run $L[h_u..t_u]$, the associated bit $B[SA[h_u - 1]] = 1$ is cleared and the corresponding difference $D[rank_1(B, SA[h_u - 1])]$ removed.

Toehold recovery. During the execution of $backwardsearch(P) = (sp_1, ep_1, SA[sp_1])$, the run ρ that determines the toehold $SA[sp_1]$ (Equation 2) may no longer retain a sample. In this case, the *sr*-index recovers $SA[h_\rho]$ by following LF steps until reaching a run head $h_{\rho'} = LF(h_\rho)^k$, with $k \leq s$, whose sample is retained ($R[\rho'] = 0$). The value is then recovered as

$$SA[h_\rho] = SA_h[rank_0(R, \rho')] + k. \quad (4)$$

Valid and invalid areas. Subsampling also affects ϕ^{-1} . Let b be the largest position such that $B[b] = 1$ and $b < SA[j]$. Equation 3 is correct iff no 1-bits were removed from the interval $B[b..SA[j]]$. Otherwise, $SA[j]$ lies in a partially valid area.

In the standard *sr*-index, the validity is detected by performing up to s LF steps starting from $j + 1$. If a run head with a retained suffix array sample is encountered, the value of $\phi^{-1}(SA[j])$ is recovered from that sample; otherwise, $B[b..SA[j]]$ is guaranteed to be valid and Equation 3 applies.

2.3.3 Fast *sr*-index variant. The standard *sr*-index always performs up to s LF steps to test validity, even when Equation 3 applies. The fast variant (Cobas et al. [6]) avoids this overhead by explicitly marking invalid areas.

Let b_a and b_{a+1} be consecutive 1-positions in the subsampled B . A bitvector V stores $V[a] = 1$ if the interval $B[b_a..b_{a+1} - 1]$ is fully valid, and $V[a] = 0$ if it is partially valid. In the latter case, a prefix remains valid, while the complementary suffix is an invalid area. An array M stores the lengths of valid prefixes in partially valid intervals. Let $b_a < b' < b_{a+1}$ be the leftmost cleared position in a partially invalid $B[b_a..b_{a+1} - 1]$ ($V[a] = 0$). The entry $M[rank_0(V, a)]$ stores $b' - b_a$.

Given a $SA[j] \in [b_a, b_{a+1} - 1]$, the operation $\phi^{-1}(SA[j])$ is computed as follows:

- (1) If $V[a] = 1$, the area is valid and Equation 3 is correct.
- (2) If $V[a] = 0$ and $b + M[rank_0(V, a)] > SA[j]$, $SA[j]$ falls within a valid prefix and Equation 3 still applies.
- (3) If $V[a] = 0$ and $b + M[rank_0(V, a)] \leq SA[j]$, then $SA[j]$ falls within an invalid area and $\phi(SA[j])$ is recovered via LF steps.

This scheme ensures that LF traversal is only used when strictly necessary, significantly reducing query time in practice.

Figure 1 illustrates the components of the *sr*-index and its fast variant.

3 The VLB-tree: an adaptive representation of the BWT

A single random edit in the text typically creates multiple new short runs in the BWT. This happens because even a local modification may change the lexicographic order of many suffixes, which ultimately determines the ordering of symbols in the BWT. As a consequence, small edits may have a disproportionate impact on the number of BWT runs r , directly increasing the space usage of the *r*-index, whose size depends on that number.

A key observation, however, is that these newly created short runs are not distributed uniformly across the BWT. In practice, some regions remain highly compressible after edits, while others become locally irregular. This phenomenon

is also reflected in the BWT's ability to benefit from block-based compression, where independent zeroth-order encoding of blocks can still achieve high-order compression [11].

The r -index does not fully exploit this property, as it treats all runs uniformly, regardless of their local density or distribution. This motivates an adaptive representation that varies its granularity according to the local distribution of runs, keeping compressible regions compact while recursively refining irregular ones.

We now introduce *variable-length blocking* (VLB) to form a hierarchical representation of the BWT that realizes this adaptive strategy (the VLB-tree). Our encoding naturally enables a more cache-friendly layout, as large compressible regions can be processed with minimal memory accesses, while irregular regions are explored only when necessary.

3.1 Overview of the VLB-tree

The VLB-tree decomposes L into blocks whose sizes adapt to the local distribution of runs:

- Compressible regions (few runs) are stored in large leaf blocks.
- Irregular regions (many runs) are subdivided recursively until their fragments have a manageable number of runs.

We begin by dividing L into n/ℓ blocks $L_1, L_2, \dots, L_{n/\ell}$ of size ℓ , processed from left to right. For each L_b , we compute $rle(L_b)$ and compare its number of runs to a threshold w , the maximum allowed in a leaf.

Compressible blocks. If $rle(L_b)$ has fewer than w runs, we try to extend it by concatenating consecutive blocks $L_b \cdots L_{b+z-1}$. We increase z while $rle(L_{b,b+z-1})$ has at most w runs and stop when $rle(L_{b,b+z})$ exceeds this threshold. The fragment $rle(L_{b,b+z-1})$ becomes a leaf superblock whose parent is the root of the tree.

Incompressible blocks. If $rle(L_b)$ has more than w runs, L_b is considered incompressible and is subdivided. Given a branching factor f , we split L_b into f equal-length parts of size $|L_b|/f$ and process them recursively from left to right using the same merging-and-splitting rule. Some parts may merge into a leaf superblock; others may subdivide further. The process adapts automatically to the local run structure.

The resulting structure places highly compressible regions close to the root, yielding small access costs, while irregular regions are recursively refined and incur access costs that reflect their local run complexity.

Recursive partitioning by a constant factor f simplifies navigation to the appropriate fragment of the BWT. Given a position $L[i]$, we compute the top-level block $b = \lceil i/\ell \rceil$, its local position $i' = i - (b-1)\ell$, and apply the same procedure recursively with block size ℓ/f until a leaf is reached.

At the same time, the formation of superblocks reduces the number of nodes and thus the space overhead. Data removed by merging blocks is recomputed on the fly by scanning up to w runs in a cache-friendly manner, which remains practical when w is small. The only problem with superblocks is that they break direct index-based access to the BWT. We restore efficient navigation by storing compact bitvectors that map positions recursively to the correct child blocks.

3.2 Layout and access in the VLB-tree

Leaves of the VLB-tree store BWT fragments, while internal nodes store routing information that enables efficient navigation to these fragments.

Let L^u denote the recursive fragment of L associated with a node u . If u is not the root, there exists a parent node v whose fragment L^v was partitioned into equal-length blocks, and where one of its blocks L_b^v corresponds to the start of L^u .

Let $\Sigma^v = [1..\sigma^v]$ be the alphabet of L^v , and let $\Sigma^u \subseteq \Sigma^v$ be the subset of symbols appearing in L^u . The operator $\text{alphacomp}(L^u)$ maps the symbols of Σ^u to the compact alphabet $[1..\sigma^u]$. Unless stated otherwise, symbols in L^u are referred to using their compacted identifiers.

Each node stores its local alphabet, which typically becomes smaller at deeper levels of the tree. Several auxiliary structures are defined with respect to Σ^u ; the first is a prefix-count array used to answer rank queries.

Thus, the first two components stored at node u are:

- A bitvector $A[1..\sigma^v]$ that sets $A[c] = 1$ if the parent symbol $c \in \Sigma^v$ appears in L^u .
- A prefix-count array $O[1..\sigma^u]$ where the symbols of Σ^u are indexed in compacted form. For each parent symbol $c \in \Sigma^v$ with $A[c] = 1$, $O[\text{rank}_1(A, c)]$ stores the number of occurrences of c in $L_{1,b-1}^v$.

The remaining components depend on whether u is a leaf or an internal node.

3.2.1 Leaves. A leaf u corresponds to a maximal fragment $L^u = L_b^v \dots L_{b+z-1}^v$, with $z \geq 1$, such that $\text{rle}(L^u)$ contains at most w runs, but including block L_{b+z}^v would exceed w runs. The leaf stores:

- An array $E = \text{rle}(\text{alphacomp}(L^u))$.

Encoding of the runs. We encode the runs in E using a space-efficient layout that supports fast scans. Each run is stored as an integer x , whose first p bits encode the run symbol and whose remaining bits encode the run length, where p depends on the local alphabet of E . The encoding applies to these integers. Our design is inspired by the vbyte-based scheme of Lemire and Boytsov [19] and enables parallel decompression, making it amenable to SIMD implementations.

We represent E as a byte stream $C_1U_1 \cdot C_2U_2 \dots C_kU_k$, where each 8-bit control byte C_k specifies the byte lengths of the runs stored in the variable-length stream U_k . The number of runs packed in each U_k depends on the largest run encoding in the leaf: eight runs if all fit in at most two bytes, four runs if up to four bytes are needed, and two runs otherwise (up to eight bytes). Accordingly, the bits of C_k encode the byte length of each run.

The number of runs packed in each C_kU_k block also determines the degree of parallel decompression. As a special case, when all runs fit in a single byte, we store E in plain format. During VLB-tree queries, SIMD instructions are used to accelerate scans of E .

3.2.2 Internal nodes. A node u is internal when its fragment $L^u = L_b^v$ contains more than w runs. In this case, we divide L^u into f equal-length parts $L_1^u, L_2^u, \dots, L_f^u$ of length $\ell_u = |L^u|/f$, and process them recursively from left to right using the same merging-and-splitting rule.

Some parts become internal nodes (if they have $> w$ runs), while other consecutive parts within the same parent may merge into leaf superblocks (if their concatenation has $\leq w$ runs).

The variable-length partition of L^u prevents direct index-based access, but we restore efficient navigation with additional routing information. Let $L^u[i]$ be a position falling within a fragment $L^e = L_{o,o+z-1}^u$ of a child e of u , with $z \geq 1$. We compute:

- The index $b = \lceil i/\ell_u \rceil$ for the block L_b^u where i falls, with $b \in [0..o+z-1]$.
- The index o for $L_{o,o+z-1}^u$. This value maps $L^u[i]$ to its position $i - (o-1)\ell_u$ within L^e .
- The child index q for e among the children of u . This information tells us what pointer to follow to visit L^e .

$$rle(L) = (\text{T}, 2)(\text{A}, 1)(\text{T}, 8)(\$, 1)(\text{C}, 3)(\text{G}, 7)(\text{A}, 6)(\$, 4)(\text{A}, 5)(\text{T}, 1)(\text{A}, 2)(\text{T}, 2)(\text{A}, 3)$$

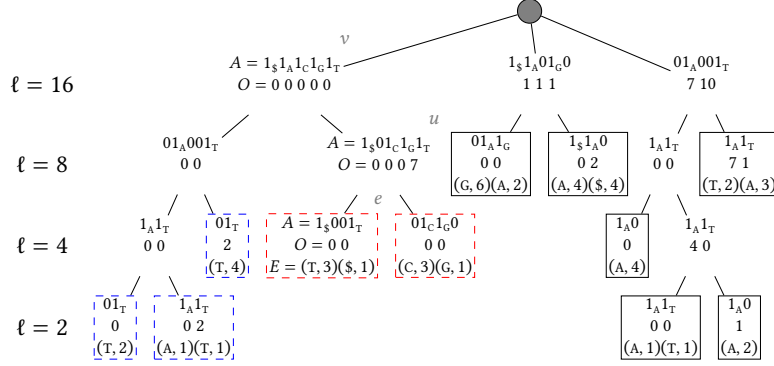


Fig. 2. VLB-tree built on the BWT L from Figure 1. The parameters are $\ell = 16$, $f = 2$, and $w = 2$. In nodes v, u, e , we label the stored node fields (omitted elsewhere for readability). We also omit array X as it is the same in all nodes ($X = 11$, no superblocks), and the pointer array P . In the alphabet bitvector A , a 1 indicates that the corresponding parent symbol appears in the node. Subscripts annotate each 1 (and the run-length sequence E) with the original text symbols. Dashed boxes correspond to Example 3.1.

Accordingly, an internal node u stores:

- A bitvector $X[1..f]$ marking which of the f parts begin a child. If $f = 4$ and $X = 1001$, then L_1^u, L_2^u, L_3^u defines the first child and L_4^u the second, so u has $f' = 2$ children.
- An array $P[1..f']$ containing pointers to the children of u .

We compute $o = \text{pred}_1(u.X, b)$, $q = \text{rank}_1(u.X, o)$, and follow the pointer $u.P[q]$ to reach e .

The branching factor f is kept small (e.g. $f \leq 64$) so that pred_1 and rank_1 in $X[1..f]$ are implemented with bitwise operations on a single machine word. Figure 2 and Example 3.1 illustrate the VLB-tree construction.

Example 3.1. The VLB-tree of Figure 2. The sequence of L is initially partitioned into $\lceil n/\ell \rceil = \lceil 45/16 \rceil = 3$ blocks L_1, L_2, L_3 . The first block $rle(L_1) = (\text{T}, 2)(\text{A}, 1)(\text{T}, 8)(\$, 1)(\text{C}, 3)(\text{G}, 1)$ has $6 > w$ runs, so we create a new internal node v . The local alphabet of L_1 has all the symbols of Σ and L_1 does not have a left context, so the alphabet bitvector is $v.A = 11111$ and the prefix-count array is $v.O = 00000$. We now build the subtree of v using $L^v = \text{alphacomp}(L_1)$ and block size $\ell = 16/2 = 8$. L^v has two parts L_1^v, L_2^v , and their compressed sequences are $rle(L_1^v) = (\text{T}, 2)(\text{A}, 1)(\text{T}, 5)$ (blue dashed boxes) and $rle(L_2^v) = (\text{T}, 3)(\$, 1)(\text{C}, 3)(\text{G}, 1)$ (red dashed boxes). Both yield internal nodes as they have more than w runs each. Assume that we have already processed L_1^v , and now we have to create an internal node u for $L^u = \text{alphacomp}(L_2^v)$. The local alphabet of L_2^v is $\Sigma^u = \{\$, \text{C}, \text{G}, \text{T}\}$, so the alphabet bitvector becomes $u.A = 10111$. From the symbols in L_2^v , only T (compact index 4) occurs in the left context L_1^v (seven times), meaning that the prefix-count array is $u.O = 0007$. The block size now becomes $\ell = 8/2 = 4$ and the rest of the tree is computed similarly.

3.2.3 The root as special case. The VLB-tree root represents the entire sequence L , and therefore does not store the prefix-count array. However, unlike internal nodes – which have at most f children – the root may have up to $\lceil n/\ell \rceil$ children. Storing the bitvector $X[1..\lceil n/\ell \rceil]$ with fast rank_1 and select_1 operations would be costly.

Instead, we use an array $P[1..\lceil n/\ell \rceil]$ that encodes both the children’s pointers and collapsed runs of zeros in X . If the (logical) bitvector X has $X[b] = 1$, then $P[b]$ stores a pointer to child $q = \text{rank}_1(X, b)$ of the root. If $X[b] = 0$, then $P[b]$ stores the offset $b - \text{pred}_1(X, b)$. The least significant bit of $P[b]$ indicates whether it is a pointer or an offset.

Algorithm 1: $access(L, i)$

```

1  $u \leftarrow$  root of the VLB-tree
2  $b \leftarrow \lceil i/\ell \rceil, o \leftarrow b$ 
3 if  $P[b]$  is an offset  $o \leftarrow b - P[b]$ 
4  $i \leftarrow i - (o - 1)\ell$ 
5  $\ell \leftarrow \ell/f$ 
6  $u \leftarrow$  node in  $u.P[o]$ 
7  $P \leftarrow \emptyset$ 
8 while  $u \neq$  leaf
9    $P \leftarrow P \cup \{u\}$ 
10   $b \leftarrow \lceil i/\ell \rceil, o \leftarrow pred_1(u.X, b), q \leftarrow rank_1(u.X, o)$ 
11   $i \leftarrow i - (o - 1)\ell$ 
12   $\ell \leftarrow \ell/f$ 
13   $u \leftarrow$  node in  $u.P[q]$ 
14  $c \leftarrow$  symbol of the run  $u.E[z]$  that contains  $i$ 
15  $c \leftarrow select_1(u.A, c)$ 
16 for  $j \leftarrow |P|$  to 1 do
17    $u \leftarrow P[j]$ 
18    $c \leftarrow select_1(u.A, c)$ 
19 return  $c$ 

```

To locate the root child covering $L[i]$, we compute the top-level block $b = \lceil i/\ell \rceil$, read $P[b]$, and either follow the pointer directly (if it is a pointer), or follow the pointer stored at $P[b - P[b]]$ (if $P[b]$ is an offset).

Although P may be larger than storing X plus rank and predecessor data structure, it keeps navigation cache-friendly.

Practical considerations. The construction of the tree uses the parameters ℓ , f , and w . We assume $\ell > w$ and that both ℓ and w are powers of f ; that is, $\ell = f^x$ and $w = f^y$ for some integers x and y . All nodes are stored in a contiguous memory region in depth-first (DFS) order. Each node's encoding is byte-aligned, so the pointers in the array P are byte offsets into this memory region.

3.3 Accessing positions of the BWT

For any position i , define $path(i) = u_1, u_2, \dots, u_l$ as the list of nodes in the VLB-tree visited to locate $L[i]$, where u_1 is the root and u_l is a leaf.

The operation $access(L, i)$ consists of three phases: a top-down descent to identify the leaf containing position $L[i]$, a local scan of the leaf to find the compacted symbol, and a bottom-up ascent to recover the original symbol in Σ .

The descent follows the navigation mechanism described in Sections 3.2.2 and 3.2.3. Starting from the root, we repeatedly use the routing information stored at each internal node to select the child fragment containing the current position and update i to its local offset within that fragment. The descent terminates at a leaf u_l such that $L[i] \in L^{u_l}$.

When the descent halts at the leaf u_l , we scan $u_l.E$ to find the leftmost run $u_l.E[z] = (c, l)$ whose cumulative length reaches i .

We then ascend along u_l, u_{l-1}, \dots, u_2 updating the compacted symbol c at each level to the corresponding parent symbol $c = select_1(u_j.A, c)$. This process yields the original $L[i]$ in Σ .

Algorithm 1 shows the process in more detail.

THEOREM 3.2. *Let \mathcal{T} be a VLB-tree built on top of the BWT L of S with parameters f , w , and ℓ . Accessing $L[i]$ in \mathcal{T} takes $O(\log_f(\ell/w) + w)$ time.*

PROOF. The total time is the height of \mathcal{T} plus the time spent scanning a leaf. During the construction of \mathcal{T} , blocks of size ℓ are repeatedly divided by a factor f until the resulting fragments have at most w runs. We choose $\ell = f^x$ and $w = f^y$ with $x > y$. A node at depth h encodes a fragment of length ℓ/f^{h-1} . These fragments range from size ℓ (children of the root) down to w (where the subdivision stops). Thus the maximum depth is $\log_f \ell - \log_f w = \log_f(\ell/w)$ nodes. Each leaf has $\leq w$ runs, which gives the additive term w . \square

The worst case arises when roughly ℓ BWT runs of length 1 occur consecutively — an uncommon situation in highly repetitive data. If i falls inside a leaf superblock attached directly to the root — a common case in repetitive inputs —, then $\text{path}(i)$ has two nodes, so the time drops to $O(w)$. Choosing a small threshold w (e.g., ≈ 64) makes the final linear scan over E effectively constant using SIMD. The number of cache misses along $\text{path}(i)$ is bounded by $\log_f(\ell/w)$ (assuming each node fits in cache), and deeper nodes exhibit better locality. A small w also keeps E cache-resident, further reducing misses.

3.4 Adding support for rank and successor

The compressed suffix array requires rank and successor queries to support pattern matching. However, implementing these operations in the VLB-tree is challenging because each node only stores information about its local alphabet, whereas the queries receive as input an arbitrary symbol c and a position i . We augment the VLB-tree to address this issue.

The operations $\text{rank}_c(L, i)$ and $\text{succ}_c(L, i)$ return different information, but they can be implemented using the same traversal strategy in the VLB-tree. We begin by following $\text{path}(i) = u_1, u_2, \dots, u_l$ and stop at the first node whose local alphabet does not contain c . At that level, the traversal diverges to a close node (typically a sibling) that leads to the answer. In the case of the rank query, this corresponds to the one leading to the closest occurrence of c to the left of i ($\text{pred}_c(L, i)$), while for the successor query, it leads to the closest occurrence of c to the right of i .

Our current encoding does not allow us to infer the diverging nodes efficiently, so we will augment the internal nodes with additional routing information to visit these paths.

Consider an internal node u corresponding to the fragment L^u . Its compacted alphabet is $\Sigma^u = [1..\sigma^u]$, and the partition of L^u induces f^u children for u . We add:

- A bitvector $N[1..f^u\sigma^u]$ storing the concatenation of σ^u bitvectors $N_1[1..f^u] \cdot N_2[1..f^u] \cdots N_{\sigma^u}[1..f^u]$. For a symbol $c \in \Sigma^u$ and the child index $q \in [1..f^u]$, $N_c[q] = 1$ iff the q -th child of u contains $c \in \Sigma^u$.

The bitvector N indicates whether the symbol c appears in each child of u , and using succ_1 and pred_1 queries on N_c redirects the traversal to the nearest left/right sibling containing c . When N_c fits a machine word, these queries run in $O(1)$ time via word operations. The additional $f^u\sigma^u$ bits per internal node impose only a small overhead because $f^u \leq f$ and the local alphabet size σ^u is small in repetitive texts and typically decreases at deeper tree levels.

The root also requires such routing information. However, the size of its corresponding bitvector can reach $\sigma(n/\ell)$ bits, too large to fit a machine word, thus requiring auxiliary data structures to support succ_1 and pred_1 . These extra structures would likely reside far from the root in memory, causing cache misses — similarly to the issue with bitvector X (Section 3.1).

To avoid this overhead, we reorganize the routing information of the root by distributing it across its children.

Algorithm 2: $rank_c(L, i)$

```

1  $u_2 \leftarrow$  root child in  $path(i)$ 
2 if  $u_2.A[c] = 0$ 
3    $y_1 \leftarrow$  node indicated by  $u_2.Z[c]$ 
4   return  $y_1.O[rank_1(y_1.A, c)]$ 
5  $r \leftarrow 0$ 
6 for  $u_j \in u_2, u_3, \dots, u_l \subset path(i)$  do
7    $c \leftarrow rank_1(u_j.A, c)$ 
8    $r \leftarrow r + u_j.O[c]$ 
9    $q \leftarrow$  child index of  $u_{j+1}$  in  $u_j$ 
10  if  $u_j.N_c[q] = 0$ 
11     $y_1 \leftarrow$  nearest left sibling of  $u_{j+1}$  with  $c$ 
12    if  $y_1 = \text{NULL}$  then return  $r$ 
13    for  $y \in y_1, y_2, \dots, y_l$  do
14       $c \leftarrow rank_1(y.A, c)$ 
15       $r \leftarrow r + y.O[c]$ 
16    return
17    $r' \leftarrow$  cum. run lengths of  $c$  in  $y_l.E$ 
18 return  $r + r'$ 

```

Algorithm 3: $succ_c(L, i)$

```

1  $u_2 \leftarrow$  root child in  $path(i)$ 
2 if  $u_2.A[c] = 0$ 
3    $y_1 \leftarrow$  node indicated by  $u_2.Z[c]$ 
4   for  $y \in y_1, y_2, \dots, y_l$  do
5      $c \leftarrow rank_1(y.A, c)$ 
6   return global idx of the first  $c$  in  $y_l.E[z]$ 
7  $c_k \leftarrow c, p_k \leftarrow u_2.Z[c]$   $\triangleright$  candidate for divergence
8 for  $u_j \in u_2, u_3, \dots, u_l \subset path(i)$  do
9    $q \leftarrow$  child index of  $u_{j+1}$  in  $u_j$ 
10   $q' \leftarrow succ_1(u_j.N_c, q + 1)$   $\triangleright$  next sib. of  $u_j$  with  $c$ 
11  if  $q' \neq \text{NULL}$  then  $c_k \leftarrow c, p_k \leftarrow u_j.P[q']$ 
12  if  $u_j.N_c[q] = 0$ 
13     $c \leftarrow c_k, y_1 \leftarrow$  node indicated by  $p_k$ 
14    execute Lines 4-6
15   $c \leftarrow rank_1(u_j.A, c)$ 
16  find the first run  $u_l.E[z]$  for  $c$  after local  $i$  in  $u_l$ 
17  if  $u_l.E[z]$  is found then return global idx its first  $c$ 
18   $c \leftarrow c_k, y \leftarrow$  node indicated by  $p_k$ 
19  execute Lines 4-6

```

For each root child u , we create:

- An array $Z[1..\sigma]$ that stores in $Z[c]$ the distance between u and its closest right-hand sibling y such that c occurs in L^y . Thus, if u and y are the children q and q' of the root (respectively), then $u.Z[c] = q' - q$.

We use Z only when redirection is required from the second node (root child) in the traversal, ensuring that the necessary routing information is local and avoiding cache misses.

The aggregate space of all Z arrays may exceed that of the root's bitvector N and its auxiliary data structures, but we adopt this design to preserve cache efficiency. In Section 5, we describe a technique to reduce the space of Z with no penalty in query time.

3.4.1 Rank algorithm. We begin the algorithm for $rank_c(L, i)$ by descending $path(i) = u_1, u_2, \dots, u_l$ as described in Section 3.3. Throughout the process, the variable c is updated to denote the compacted symbol corresponding to the current node.

Root-child special case. If $u_2.A[c] = 0$, the fragment L^{u_2} does not contain c , so we visit the right-hand sibling y_1 indicated by $u_2.Z[c]$ and report the prefix count from $y_1.O[c]$. Node y_1 lies on $path(succ_c(L, i))$, not on $path(pred_c(L, i))$, which we previously stated would be used for $rank_c$. However, the answer in $y_1.O$ is still correct because it considers the occurrences of c preceding L^{u_2} . This is exceptional because $u_2.Z$ does not provide information for redirecting to a left-hand sibling.

General internal node. This case assumes $u_2.A[c] = 1$. For an internal node $u_j \neq u_2$ with child index q for u_{j+1} , if $u_j.N_c[q] = 0$, then u_{j+1} does not contain c . We therefore compute $y_1 = pred_1(u_j.N_c, q - 1)$, the closest left-hand sibling of u_{j+1} that contains c . If there is no y_1 , we return the cumulative prefix count for c collected up to u_j . If y_1 exists, we

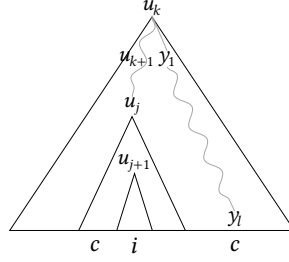


Fig. 3. Finding the successor node containing c .

descend the rightmost branch y_1, y_2, \dots, y_l that contains c , computing each successive child as $y_{j+1} = \text{pred}_1(y_j.N_c, f^{y_j})$, where f^{y_j} is the number of children for y_j . Upon reaching the leaf y_l , we scan its entire sequence $y_l.E$, count all occurrences of c , and add them to the cumulative rank for c along the nodes u_2, \dots, u_j and the redirected branch y_1, \dots, y_l . The full leaf scan is necessary since the subtree of y_1 lies entirely before position i , so all occurrences in y_l contribute to rank. The final rank value is the answer for $\text{rank}_c(L, i)$.

Algorithm 2 illustrates the procedure.

3.4.2 Successor algorithm. As mentioned above, $\text{succ}_c(L, i)$ operates almost the same way as $\text{rank}_c(L, i)$. The most notable change is the node we search after diverging. The query returns a null value if no valid successor for c exists in $L[i..n]$.

We descend $\text{path}(i)$, compacting c accordingly, until we reach the first node u_j where u_{j+1} does not contain c ($u_j.N_c[q] = 0$). From there, we locate the deepest ancestor $u_k \in \text{path}(i)$, with $k \leq j$, such that L^{u_k} has an occurrence of c to the right of the local i .

Once we locate u_k , we move to the closest right-hand sibling y_1 of u_{k+1} , and continue descending the leftmost branch y_1, y_2, \dots, y_l that contains c . The initial compacted symbol is c_k and each subsequent node y_{j+1} is the leftmost child of y_j that contains c . Upon reaching y_l , the algorithm scans $y_l.E$ until it finds the first run $y_l.E[z]$ for c , and reports the index in L for the first c in $y_l.E[z]$ (i.e., its global index). Figure 3 illustrates the divergence mechanism.

If no stopping node u_j is found and the descent of $\text{path}(i)$ reaches its leaf u_l , the algorithm scans $u_l.E$ to locate the first run $u_l.E[z]$ of c such that the cumulative run length is equal to or greater than the local i . If such a run exists, it returns its global index in L . If the run does not exist, c does not occur in suffix $L^{u_l}[i..]$, so the algorithm follows the leftmost branch of y_1 as described before.

Finding the branching node. To avoid backtracking $\text{path}(i)$ to find u_k , during descent, we maintain, for each internal node $u_j \in \text{path}(i)$ with $j \geq 2$, a pointer p_k to a candidate redirection node y_1 together with the compacted value c_k of c in $\text{alphacomp}(L^{u_j})$.

For a root child u_2 , p_k is $u_2.Z[c]$ and $c_k = c$ (or null if no valid successor exists). For a general internal node $u_j \neq u_2$ where the child index for u_{j+1} is q , p_k points to the next right-hand sibling $\text{succ}_1(u_j.N_c, q+1)$ containing c and c_k is the compacted c in u_j . If no valid pointer p_k is found (i.e., u_{j+1} does not have a right-hand sibling for c), the pair (p_k, c_k) is inherited from u_{j-1} .

Once the stopping node u_j is found, the algorithm moves to the node y_1 indicated by p_k , updates $c = c_k$, and starts the descent of the leftmost branch for c in y_1 . On the other hand, if p_k is a null pointer, $\text{succ}_c(L, i)$ returns a null value.

Algorithm 3 shows the successor mechanism in more detail.

A modified successor query. The operation $\text{backwardsearch}(P) = (sp_1, ep_1, SA[sp_1])$ internally uses a variant of $\text{succ}_c(L, i) = h_\rho$ that returns the index ρ of the run $L[h_\rho..t_\rho]$ where h_ρ lies. This index indicates the suffix sample $SA_h[\rho]$ from which the toehold $SA[sp_1]$ is derived (Equation 2). Our VLB-tree design will distribute SA_h in the leaves to improve cache efficiency (Section 4) so an index ρ does not necessarily tell where $SA_h[\rho]$ is stored. We define a more convenient query:

- $\text{msucc}_c(L, i)$: Let $\text{succ}_c(L, i) = i'$ be a successor index for c and let $L[h_\rho..t_\rho]$ be the run where i' falls in L . The *memory successor* query $\text{msucc}_c(L, i)$ returns the byte offset within the VLB-tree where $SA_h[\rho]$ resides.

Theoretical cost. We note that the theoretical cost of the rank and successor algorithms remains the same as that of $\text{access}(i)$ (Section 3.3), and they incur $O(\log_f(\ell/w))$ additional cache misses if they have to diverge the traversal.

4 Counting with toehold

The current VLB-tree encoding (Section 3.4) already supports the query $\text{rank}_c(L, i)$, which is sufficient to compute the backward-search intervals (sp_l, ep_l) using Equation 1. The next step is to use Equation 2 to obtain the toehold $SA_h[sp_1]$. We need:

- To determine the step g and its position sp_g .
- To retrieve $SA_h[\rho]$ given g and sp_g .

We describe how to support both operations in the VLB-tree.

4.1 The step for the toehold

Cobas et al. [6] present a simple method to obtain g and sp_g : initially, set $g = m + 1$ and $sp_g = 1$, and run the backward search. Whenever a step (sp_l, ep_l) satisfies $L[sp_l] \neq P[l - 1]$, update $g = l$ and $sp_g = sp_l$. The final values are obtained once (sp_1, ep_1) is reached.

The challenge is to test $L[sp_l] \neq P[l - 1]$ in a cache-friendly manner because Equation 1 does not necessarily visit the area for $L[sp_l]$. We define a new query $\text{headrank}_c(L, i) = (o, b)$ in the VLB-tree, where o is the number of occurrences of c in $L[1..i]$ and b is a bit set to 1 if $L[i] = c$.

This operation behaves like $\text{rank}_c(L, i)$ (Section 3.4.1), with one additional check:

- If $\text{path}(i)$ diverges from $\text{path}(\text{pred}_c(L, i))$, then $L[i] \neq c$ and we set $b = 0$.
- Otherwise, both paths coincide. Let v be the leaf reached and let i' be the local position of i in L^v . We set $b = 1$ if $L^v[i']$ matches c , and $b = 0$ otherwise.

A subtle issue arises because Equation 1 infers $sp_{l-1} = C[P[l - 1]] + \text{rank}_{P[l-1]}(L, sp_l - 1) + 1$, whereas we now perform rank at position sp_l . Since $L[sp_l - 1]$ and $L[sp_l]$ may lie in different fragments of the VLB-tree, we adjust the computation as follows.

We first run $\text{headrank}_{P[l-1]}(L, sp_l) = (o, b)$. If $b = 1$, we decrement o by one; otherwise, o is left unchanged. The value $sp_{l-1} = C[P[l - 1]] + o + 1$ is therefore identical to the original formulation.

4.2 Suffix array samples

After computing g and sp_g , we must retrieve the index ρ such that $\text{succ}_{P[g-1]}(L, sp_g) = h_\rho$. The VLB-tree query $\text{succ}_{P[l-1]}(L, sp_g)$ (Section 3.4.2) returns the index h_ρ , but this alone does not identify where $SA_h[\rho]$ is stored.

We address this by augmenting the leaves of the VLB-tree with suffix array samples. For a leaf v whose sequence $v.E$ contains m' runs, we store an array $W[1..m']$ such that $W[z]$ equals the value of SA_h associated with the z -th run of $v.E$ (from left to right).

With this structure in place, retrieving $SA_h[\rho]$ is straightforward. Given g and sp_g , we call $msucc_{P[g-1]}(L, sp_g)$ (Section 3.4) to obtain the leaf v containing the BWT position h_ρ . Let $v.E[z]$ be the run where h_ρ lies; the desired suffix array sample is $v.W[z] = SA_h[\rho]$.

A key advantage of this design is that $msucc_{P[g-1]}(L, sp_g)$ and the subsequent retrieval of $SA_h[w]$ are performed in the same memory area (the leaf v), ensuring excellent locality. In contrast, traditional r -index implementations store SA_h and L in different memory locations.

Handling run splitting. Because the tree construction may split BWT runs across leaves, the first and last elements of $v.E$ may be *partial*. In particular, $v.E[1]$ is partial if the symbol preceding L^v in L is the same as the symbol of $v.E[1]$. Each leaf stores a flag indicating whether this situation occurs.

When $v.E[1]$ is partial, its corresponding BWT area is a proper suffix $L[t_\rho - q + 1..t_\rho]$ of a run $L[h_\rho..t_\rho]$. Since the values of SA_h are associated with run heads, and $v.E[1]$ does not include $L[h_\rho]$, the array $v.W$ does not have a value for $v.E[1]$. In this case, each entry $v.W[z]$ corresponds to $v.E[z+1]$.

This situation does not affect the retrieval of $SA_h[\rho]$. The positions sp_g and h_ρ always belong to different BWT runs. Consequently, if h_ρ lies in the run $v.E[z]$ of some leaf v , then $v.E[z]$ cannot be partial and $v.W$ is guaranteed to have a sample for h_ρ .

5 Reducing the space usage of the VLB-tree

A drawback of the VLB-tree that we have not yet addressed is the space overhead introduced by the satellite data stored at the root level. Each child u_2 of the root stores an array Z , which allows the traversal of $path(i) = u_1, u_2, \dots, u_l$ to jump to an appropriate right-hand sibling whenever a divergence is required. This information is used when answering both rank and successor queries (Section 3.4). Since the root may have up to n/ℓ children and each Z array has σ entries, the space overhead can reach $\sigma(n/\ell)$ bits in the worst case.

In this section, we show how to reduce this cost by sampling each array Z while still ensuring that the operation $backwardsearch(P[1..m])$ works correctly whenever P occurs in S . When P is not in S , operations *rank*, *headrank*, and *msucc* may fail, returning zero or null when they should return a non-zero or non-null value. This behavior is acceptable, since this function naturally returns an empty range ($sp_1 > ep_1$) when P does not appear in S .

Intuition. Each array Z does not need to store entries for *all* symbols in Σ . Consider the suffix array range $SA[sp_l..ep_l]$ representing the suffixes of S prefixed by $P[l..m]$. The next backward-search step computes $rank_{P[l-1]}(L, sp_l)$ (or *headrank* in our case) to obtain sp_{l-1} . However, if the pattern $P[l-1..m]$ does not exist in S , there is no need to store an entry for $P[l-1]$ in the array Z of the root child u_2 containing position sp_l . We now formalise this idea.

Let $\mathcal{S} \subset \{(s, e) \in [n] \times [n] \mid s \leq e\}$ be the set of valid ranges² in SA that $backwardsearch(P)$ may visit when computing $(sp_1, ep_1) \in \mathcal{S}$ for any pattern P in S .

For a pair (p, q) with $1 \leq p \leq q \leq n$, define

$$\begin{aligned}\mathcal{L}(p, q) &= \{(s, e) \in \mathcal{S} \mid s \leq p \leq e \leq q\} \text{ and} \\ \mathcal{R}(p, q) &= \{(s, e) \in \mathcal{S} \mid p \leq s \leq q \leq e\},\end{aligned}$$

²For readers familiar with suffix trees, \mathcal{S} contains the ranges associated with the nodes of the suffix tree of S .

representing the sets of suffix array ranges overlapping the left and right ends of (p, q) , respectively. The *leftmost* and *rightmost* overlaps of (p, q) are

$$\begin{aligned} lmo(p, q) &= \arg \min_{(s, e) \in \mathcal{L}(p, q)} s \text{ and} \\ rmo(p, q) &= \arg \max_{(s, e) \in \mathcal{R}(p, q)} e, \end{aligned}$$

respectively, breaking ties for $lmo(p, q)$ by choosing the pair with the largest e , and for $rmo(p, q)$, the pair with the smallest s .

For a BWT substring $L[p..q]$ and its overlapping suffix array ranges $(a, b) = lmo(p, q)$ and $(y, z) = rmo(p, q)$, let $\Sigma^{(a, p-1)} \subseteq \Sigma$ and $\Sigma^{(q+1, z)} \subseteq \Sigma$ be the alphabets of $L[a..p-1]$ and $L[q+1..z]$, respectively.

LEMMA 5.1. *Let u_2 be a root child in the VLB-tree with fragment $L^{u_2} = L[p..q] \in \Sigma^*$. The array $u_2.Z$ can be sampled so that it stores entries only for symbols in $\Sigma^{(a, p-1)} \cup \Sigma^{(q+1, z)}$, and $\text{backwardsearch}(P)$ still returns the correct result whenever P occurs in S .*

PROOF. Let $l \in \{m+1, m, \dots, 2\}$ be a step in the operation $\text{backwardsearch}(P)$, and let $SA[sp_l..ep_l]$ be the range of suffixes in S prefixed by $P[l..m]$. We say that the triple $(sp_l, ep_l, P[l-1])$ is *valid* if $P[l-1]$ occurs in $L[sp_l..ep_l]$, which is equivalent to $P[l-1..m]$ occurring in S .

To prove the lemma, it suffices to show that whenever a rank or successor operation in $\text{backwardsearch}(P)$ process a valid index $i \in [p..q]$ and a valid symbol c , the sampled array $u_2.Z$ contains an entry for c . Indeed, a valid triple $(sp_l, ep_l, P[l-1])$ produces a range (sp_{l-1}, ep_{l-1}) for a suffix $P[l-1..m]$ that exists in S .

We focus on $\text{rank}_c(L, i)$ and $\text{headrank}_c(L, i)$; the argument for the successor queries is analogous.

For an index $i \in [p, q]$, the query $\text{rank}_c(L, i)$ traverses $\text{path}(i) = u_1, u_2, \dots, u_o$ and may diverge if $\text{path}(\text{pred}_c(L, i)) \neq \text{path}(i)$. Furthermore, when $L^{u_2} = L[p..q]$ does not have occurrences of c , the algorithm falls into a special root-child case and redirects the traversal from u_2 to the right-hand sibling y_1 containing $L[\text{succ}_c(L, i)]$. The pointer to y_1 is stored in $u_2.Z[c]$ (Section 3.4.1).

Two cases must be considered when sampling $u_2.Z$.

Case one:

$$i = sp_l \text{ and } p \leq sp_l \leq q.$$

In the VLB-tree, $\text{backwardsearch}(P)$ uses $\text{headrank}_{P[l-1]}(L, sp_l)$ to compute sp_{l-1} . It may happen that $P[l-1]$ does not occur in $L[p..q]$ but does occur in $L[q+1..ep_l]$, forcing the use of $u_2.Z[P[l-1]]$. Since $(sp_l, ep_l, P[l-1])$ is valid, the entry $u_2.Z[P[l-1]]$ must exist in the sampling of $u_2.Z$, otherwise $\text{backwardsearch}(P)$ fails with a pattern that exists in S . The sampling of $P[l-1] \in \Sigma^{(q+1, z)}$ is guaranteed because $(sp_l, ep_l) \in \mathcal{R}$ overlaps the right end of (p, q) , and $(y, z) = rmo(p, q)$ contains all elements of \mathcal{R} .

Case two:

$$i = ep_l \text{ and } p \leq ep_l \leq q$$

In this case, $\text{backwardsearch}(P)$ uses $\text{rank}_{P[l-1]}(L, ep_l)$ to compute ep_{l-1} . The symbol $P[l-1]$ may occur in $L[sp_l..p-1]$ but not in $L[p..q]$, again forcing the use of $u_2.Z[P[l-1]]$. This time, the existence of $P[l-1]$ in the sample of $u_2.Z$ is guaranteed because $(sp_l, ep_l) \in \mathcal{L}$ overlaps the left end of $L[p..q]$, and $(a, b) = lmo(p, q)$ contains all elements of \mathcal{L} .

In conclusion, a sample of $u_2.Z$ that stores information for $\Sigma^{(a, b)} \cup \Sigma^{(y, z)}$ is sufficient to ensure that $\text{backwardsearch}(P)$ is answered correctly whenever P exists in S . Figure 4 and Example 5.2 illustrates both cases and the corresponding overlaps within $L[p..q]$. \square

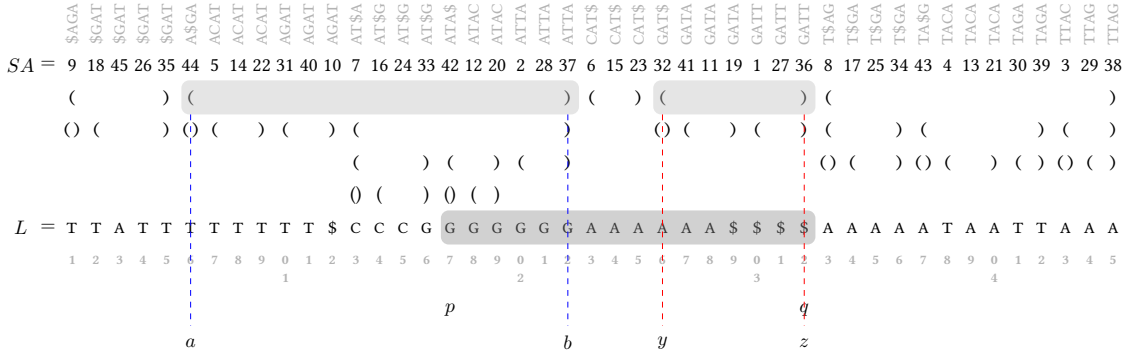


Fig. 4. Sampling of Z arrays. The parentheses are the ranges $SA[sp_1..ep_1]$ that $\text{backwardsearch}(P)$ can visit for patterns of length ≤ 4 . The gray block $L[p..q] = L[17..32]$ marks the fragment of a root child (the one in the middle in Figure 2). The gray parentheses to the left highlight the longest left overlap $(a, b) = lmo(p, q)$, and the gray parentheses to the right highlight the longest right overlap $(y, z) = rmo(p, q)$. The alphabet $\Sigma^{(a,p-1)}$ is $\{\$\text{, C, G, T}\}$ and the alphabet $\Sigma^{(q+1,z)}$ is \emptyset . The Z array for the root child encoding $L[p..q]$ thus stores pointers for $\{\$\text{, C, G, T}\}$.

Example 5.2. Performing rank with the sampling of Figure 4. Consider $\text{rank}_c(L, ep_1)$ for $c \in \{\$\text{, C, T}\}$, where $ep_1 = b$. Since c does not occur in $L[p..b]$ (and $p \leq b \leq q$), the VLB-tree uses the Z array of the root child encoding $L[p..q]$. By Lemma 5.1, c has a pointer in Z , so the query returns a valid answer. Note that $\text{rank}_A(L, b)$ returns 0 although the correct value is 1 (due to $L[3] = A$). This inconsistency is harmless because A does not occur in $L[sp_1 = a..ep_1 = b]$, so the corresponding backward-search step correctly yields an empty range ($sp_{l-1} > ep_{l-1}$).

6 Locating from toehold

In this section, we introduce a new representation for the function ϕ^{-1} used by $\text{locate}(P) = SA[sp_1..ep_1]$ to decode the suffix array values in $SA[sp_1 + 1..ep_1]$ from the toehold $SA[sp_1]$ (Section 2.3.1). This new encoding balances speed and space using adaptive techniques based on the VLB-tree.

The classical data structure for ϕ^{-1} uses a bitvector $B[1..n]$ marking text positions that correspond to run tails in the BWT, together with an array $D[1..r]$ storing suffix array differences at run boundaries. The operation $\phi^{-1}(SA[j]) = SA[j + 1]$ is then solved using Equation 3.

This formulation reveals two opportunities for improvement:

- The distribution of 1s in B is typically skewed, so adaptive structures improve space usage.
- Interleaving B, D improves spatial locality when answering $\phi^{-1}(SA[j])$.

We combine these observations by introducing a VLB-tree for ϕ^{-1} , denoted \mathcal{T}_ϕ .

6.1 The VLB-tree for locating

The tree \mathcal{T}_ϕ is built over a logical sequence $Q[1..n]$ that interleaves the information of B and D . Let b_1, b_2, \dots, b_r be the positions in B such that each $B[b_a] = 1$, and let $d_a = b_{a+1} - b_a$ denote the distance between consecutive 1s (with $d_r = n + 1 - b_r$). We define the run-length encoding of Q as

$$rle(Q) = (D[1], d_1)(D[2], d_2), \dots, (D[r], d_r),$$

where each pair $(D[a], d_a)$ forms a run, analogous to those in the BWT. The entry in $D[a]$ is the run symbol and d_a the run length.

We construct \mathcal{T}_ϕ from Q following the same principles as in Section 3.1, but storing only the information required to answer the operation $access(Q, SA[j])$. Specifically, each internal node u stores only the bitvector $u.X$ marking the superblocks and the array $u.P$ of the child pointers, while each leaf only stores the run-length sequence E corresponding to a substring of Q .

Supporting $access(Q, SA[j]) = D[rank_1(B, SA[j])]$ is sufficient to answer

$$\phi^{-1}(SA[j]) = SA[j] + access(Q, SA[j]).$$

In the description of $\phi^{-1}(SA[j])$ in Section 2.3.1, positions $SA[j]$ that fall within $B[b_a..b_{a+1} - 1]$ access $D[a]$. This range is represented in \mathcal{T}_ϕ by the run $(D[a], d_a)$, thereby improving spatial locality compared to traditional r -index implementations.

Handling run splitting. The construction of \mathcal{T}_ϕ may divide a run $(D[a], d_a)$ into several parts $(D[a], d_{a,1}), (D[a], d_{a,2}), \dots$ depending on the block size ℓ and the run length d_a . However, this partition does not affect the output of ϕ^{-1} because all positions $B[b_{a,2}], B[b_{a,3}], \dots$ are associated with $D[a]$. This property follows directly the definition of the BWT (see Section 2.3.1).

Figure 5 illustrates the construction of \mathcal{T}_ϕ .

6.1.1 Complexity and adaptivity. The traversal of $path(SA[j])$ in \mathcal{T}_ϕ allows us to find the run $(D[a], d_a)$ containing position $SA[j]$, which we then use to answer $access(Q, SA[j])$. This operation takes $O(\log_f(\ell/w) + w)$ time, ℓ , w , and f being the VLB-tree parameters.

Areas of Q containing long runs (respectively, sparse regions of B) generate leaves in \mathcal{T}_ϕ that are close to the root, resulting in fewer cache misses and short leaf scans. Conversely, regions with many short runs (equivalently, dense regions of B) are placed deeper in \mathcal{T}_ϕ , increasing space usage, but matching the inherently higher cost of navigating many runs. This adaptive behavior mirrors that of the VLB-tree used for the BWT and achieves a balanced trade-off between space and query performance.

7 Fast subsampled index

The VLB-trees for the BWT and for ϕ^{-1} together form a compressed suffix array supporting the queries $count(P)$ and $locate(P)$. However, storing the $2r$ suffix array samples required by these structures can be expensive for repetitive texts with many small variations.

The sr -index solves the space issue, but existing implementations suffer from poor cache locality because queries must traverse multiple disconnected structures (Section 2.3.2). In this section, we show how to encode both the sr -index and its fast variant (Section 2.3.3) within the VLB-tree framework, improving locality while preserving their space.

7.1 Modifications on the VLB-tree of the BWT

Let \mathcal{T}_L denote the VLB-tree of the BWT. Each leaf v in \mathcal{T}_L stores a run-length encoded fragment $v.E[1..m']$ of L and an array $v.W[1..m']$ with the suffix array samples in SA_h associated with $v.E$ (Section 4.2). After subsampling, $v.W$ shrinks if some of the runs in $v.E$ do not retain a sample.

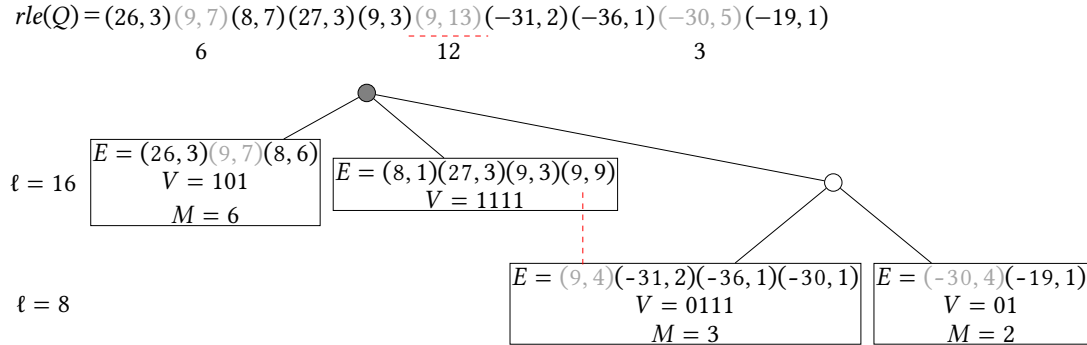


Fig. 5. VLB-tree \mathcal{T}_ϕ of the sequence Q generated from subsampled B and D of Figure 1. The parameters are $\ell = 16$, $f = 2$ and $w = 4$. Gray elements in $rle(Q)$ are partially valid areas. The number below is the length of the prefix that remains valid (gray regions in B of Figure 1). Bitvector V and array M are elements of the fast sr-index (Section 7). Dashed lines correspond to Example 7.1.

To represent this situation, we augment each leaf with a bitvector $v.R[1..m']$, where $v.R[z] = 0$ indicates that $v.E[z]$ retains its sample and $v.R[z] = 1$ otherwise. For a run $v.E[z]$ with $v.R[z] = 0$, its sample is stored at $v.W[rank_0(v.R, z)]$.

Since $m' \leq m$ and $v.R$ fits in a machine word, $rank_0$ can be computed in constant time using bitwise operations.

Backward search. The only query in \mathcal{T}_L that requires a modification is $backwardsearch(P) = (sp_1, ep_1, SA_h[sp_1])$. The run ρ in L used to derive the toehold $SA_h[sp_1]$ (Equations 2) may not retain a subsample, in which case we need to recover it (Equation 4). We operate as follows: after completing the backward search and obtaining (g, sp_g) , we use $msuccp_{[g-1]}(L, sp_g)$ to access the VLB-tree leaf v encoding the run $L[h_\rho..t_\rho]$ associated with $SA_h[\rho]$. Let $v.E[z]$ be run for $L[h_\rho..t_\rho]$. If $v.R[z] = 0$, we return $v.W[\text{rank}_0(v.R', z)] = SA_h[\rho]$, otherwise we recover $SA_h[\rho]$ via LF starting from h_ρ , as in Equation 4.

7.2 Modifications on the VLB-tree of locating

In the standard *sr*-index, the query $\phi^{-1}(SA[j])$ performs up to s *LF* steps to check if $SA[j]$ falls in valid area. A failed test indicates invalid area but returns $SA[j + 1]$ altogether, whereas a successful test does not give the answer but indicates that Equation 3 with subsampled B and D returns the correct $SA[j + 1]$ (Section 2.3.2).

This functionality does not require any modification to the VLB-tree \mathcal{T}_ϕ . We can build it directly over the logical sequence Q derived from the subsampled B and D .

On the other hand, the fast variant of the sr -index marks the invalid areas to save computations (Section 2.3.3) and therefore we must incorporate this information into the VLB-tree \mathcal{T}_ϕ .

A run $(D[a], d_a)$ in Q represents a range $B[b_a..b_{a-1} - 1]$ that is fully or partially valid. The run $(D[a], d_a)$ of a partially valid range can be split into two halves $d_{a,l}, d_{a,r}$. Let $b_a < b' < b_{a+1}$ be the leftmost cleared position within $B[b_a..b_{a+1} - 1]$ during subsampling. The left half $d_{a,l}$ refers to the valid prefix $B[b_a..b' - 1]$ while $d_{a,r}$ refers to the invalid suffix $B[b'..b_{a+1} - 1]$. In the VLB-tree of \mathcal{T}_ϕ , a query $access(Q, SA[j])$ such that $SA[j]$ falls within $d_{a,l}$ must return $D[a]$, while a query that falls in $d_{a,r}$ must return null to indicate an invalid area. A query within a fully valid area always returns the corresponding difference value in D .

We incorporate this information into \mathcal{T}_ϕ using analogous structures to those of the fast *sr*-index, augmenting each leaf with:

- A bitvector $v.V[1..m']$, where $v.V[z]$ indicates the partial or full validity of the run $v.E[z]$, and
- An array $v.M[1..rank_0(v.V, m')]$ that stores in $v.M[rank_0(v.V, z)]$ the valid prefix d_l of a partially valid run $v.E[z]$.

Handling run splitting. The only relevant consideration when building \mathcal{T}_ϕ is the update of $d_{a,l}$ when a partially valid run $(D[a], d_a)$ is split into multiple VLB-tree leaves. Suppose the construction algorithm partitions $(D[a], d_a)$ into p fragments $(D[a], d_{a,1}), (D[a], d_{a,2}), \dots, (D[a], d_{a,p})$. If the fragment $(D[a], d_{a,j})$ is contained within the prefix $d_{a,l}$ of $(D[a], d_a)$, then $(D[a], d_{a,j})$ becomes fully valid. On the other hand, if $(D[a], d_{a,j})$ is contained within the prefix $d_{a,r}$ of $(D[a], d_a)$, the fragment becomes fully invalid. Finally, when $(D[a], d_{a,j})$ falls within a substring that overlaps d_l and d_r , it remains partially valid, but its valid prefix must be updated.

Figure 5 shows examples of $v.V$ and $v.M$, and Example 7.1 illustrates the splitting of runs.

Example 7.1. In Figure 5, the run $rle(Q)[6] = (9, 13)$ (red dashed underline) corresponds to $Q[23..35]$ (equivalently, $B[23..35]$), with associated difference value 9 in D . The run is partially valid, with valid prefix length 12. During the construction of \mathcal{T}_ϕ , the run is divided into two parts, $(9, 9)$ and $(9, 4)$ (vertical dashed red line). The fragment $(9, 9)$ becomes fully valid because it lies within the valid prefix, while $(9, 4)$ remains partially valid and its valid prefix becomes $12 - 9 = 3$. Accessing $Q[23..34]$ in \mathcal{T}_ϕ returns 9, whereas accessing $Q[35]$ (the invalid suffix) returns a null value.

8 Experiments

We implemented our data structures in a C++ library called VLBT (<https://github.com/ddiazdom/VLBT>). The VLB-tree representation of the BWT (Section 3.4) is denoted `vlbt-bwt` and supports `count` queries. The compressed suffix array that combines the BWT and ϕ^{-1} VLB-trees with fast subsampling (Section 7) is denoted `vlbt-sri-va` and supports both `count` and `locate` queries. Both implementations rely on SIMD instructions to accelerate scans over run-length encoded sequences.

8.1 Experimental setup

We evaluate the tradeoffs between query speed, cache efficiency, and index size for BWT-based data structures supporting `count` and `locate` queries.

We fixed the VLBT parameters $w = 64$ and $f = 4$ to implement the operations `rank1`, `select1` and `pred1` using bitwise operations on 64-bit machine words. Then, we built multiple variants of `vlbt-bwt` and `vlbt-sri-va` by varying the block size ℓ from $4^6 = 4,096$ to $4^9 = 262,144$. In all `vlbt-sri-va` instances, the VLB-trees of L and ϕ^{-1} used the same block size ℓ , and for each block size, we varied the subsampling rate s across values 4, 8, 16, 32. A variant named `vlbt-sri-va-x` corresponds to $\ell = 4^x$, where $x \in \{6, 7, 8, 9\}$.

8.1.1 Competitor tools and measurements. We compared our VLBT variants against the following implementations:

- `mn`³: the run-length BWT of Mäkinen and Navarro [21] as implemented in [14].
- `fbb`⁴: BWT encoding using fixed block boosting [15].
- `move-count` and `move-loc`⁵: optimized implementations [2] of the move structure [23]. The variant `move-count` encodes only the BWT, while `move-loc` also includes r -suffix array samples.

³https://github.com/simongog/sdsl-lite/blob/master/include/sdsl/wt_rlmn.hpp (release 2.1.1)

⁴<https://github.com/dominikkempa/faster-minuter> (commit 9238178)

⁵<https://github.com/LukasNalbach/Move-r> (commit bed2fe9)

Dataset	Size (GB)	Alphabet	n/r	Longest run (MB)
BAC	133.12	7	116.77	0.23
COVID	267.41	17	940.49	4.11
HUM	241.24	7	61.82	6.66
KERNEL	54.45	190	263.11	70.6

Table 1. Datasets.

- `ri`⁶: the original r -index [12].
- `sri-va`⁷: the original s -index with valid ϕ^{-1} areas [6] (i.e., fast variant). We varied the sampling s across values 8, 12, 16, 20.

We created a standard command line interface to measure the speed performance of `count` and `locate` queries in run-length BWTs and r -index implementations. We excluded `move-count` and `move-loc` because its codebase is substantially more involved, and used their own interface. All interfaces receive as input an index and a set of patterns, and report the average speed for `count` and/or `locate`. The source code for these interfaces can be found in the folder `test_suite` in the VLBT repository.

We split the experiments according to the supported query types. For structures that support only `count`, we evaluated `vlbt-bwt` with `mn`, `fbb`, and `move-count`. For structures that support `count` and `locate`, we evaluated `vlbt-sri-va` against `move-loc`, `ri`, and `sri-va`.

Comparisons for vlbt-bwt. For `count` queries, we identified the fastest and the slowest `vlbt-bwt` variants and compared their query times against the other methods, reporting the resulting time range. We did the analogous comparison for space by taking the smallest and the largest `vlbt-bwt` variants. Section 8.2 summarizes these ranges.

Comparisons of vlbt-sri-va. Here, performance depends on two parameters: block size and subsampling. For each fixed block size in `sri-va`, we averaged query time (and space) over the tested subsampling values, and then reported the best-worst range across block sizes when comparing against other tools. Since `sri-va` also varies sampling, we likewise averaged its query time and space over its sampling values. When comparing `vlbt-sri-va` and `sri-va` directly, we used averages computed over the same subsampling values. Section 8.3 presents the results.

The tradeoffs of query-time versus space usage of all experiments are reported in Figure 6.

To assess cache efficiency, we measured the average number of L1 data cache misses per query symbol. For `count` queries, we compared `vlbt-bwt`, `mn`, and `fbb`; for `count` and `locate` queries, we compared `vlbt-sri-va`, `ri`, and `sri-va`. For each tool, we generated an executable that loads the index, executes queries, and records cache misses. This required special compilation steps described in Section 8.1.3. Due to compilation constraints, we could not include `move-count` and `move-loc` in the cache experiments. Results are shown in Figure 7.

8.1.2 Datasets, queries, and indexing. We built all indexes on four datasets with varying degrees of repetitiveness. Table 1 summarizes the main characteristics of the collections.

- BAC: genome assemblies of 30 bacterial species from the AllTheBacteria collection [17]. Strings belonging to the same species are highly repetitive, while strings from different species are dissimilar.

⁶<https://github.com/nicolaprezza/r-index> (commit 7009b53)

⁷<https://github.com/duscob/sr-index> (commit f99b54a)

- COVID: 4,494,508 SARS-CoV-2 genomes downloaded from the NCBI genome portal⁸. These sequences are short and near-identical, with an average length of 29,748.
- HUM: genome assemblies of 40 individuals from the Human Pangenome Reference Consortium (HPRC) [28]. Individual genomes are near-identical, but assembly differences introduced variability.
- KERNEL: 2,609,417 versions of the Linux kernel repository⁹. This dataset is highly repetitive and has a large alphabet.

In DNA collections (BAC, COVID, and HUM), we also considered the DNA reverse complement of each string (as is standard in bioinformatics). The numbers presented in Table 1 already consider these extra sequences.

We sampled 50,000 random patterns of length 105 from each dataset for the *count* experiments. For *locate* queries, we restricted the evaluation to patterns with fewer than 50,000 occurrences in the dataset to limit computational cost. For *count* queries, we report the average time (in μ secs) per pattern, computed as the total time over all queries divided by the number of queries. For *locate*, we report the average time (also in μ secs) per reported occurrence, computed as the total time divided by the number of reported occurrences returned by the queries.

We did not measure index construction time, as the compared tools rely on different building strategies and optimizations, making a fair comparison difficult and beyond the scope of this work. To ensure consistent query results, all indexes were built using BWTs and suffix array samples generated by the same tool, *bigBWT* [3].

8.1.3 Machine and compilation. All experiments were conducted on a machine running SUSE Linux Enterprise Server 15, equipped with 1 TB of RAM and an AMD EPYC 7713 processor at 2 GHz with 128 cores. No other relevant processes were running at the time we performed our measurements.

The tools were compiled using gcc 13.3 with optimization flag -O3. Our VLBT implementations use SIMD instructions from the SSE4.2 instruction set, enabled via the -msse4.2 compilation flag.

We measured cache misses using the Cray Programming Environment (CPE), which provides access to hardware performance counters. We compiled the executables for the cache experiments (one per competitor tool) using Cray clang 18.0.1 and set the environment variable PAT_RT_PERFCTR=PAPI_L1_DCM to record L1 data cache misses during query execution. Finally, we instrumented each executable using pat_build, producing executables with the +pat suffix that were used to collect the measurements.

Each executable receives as input a data structure and a set of patterns. First, it warms up the data structure by executing a sequence of random queries. This step ensures that no page faults occur when performing real cache measurements. The executable then pollutes the L1 data cache with random bits to force a cold-cache state. Finally, it executes the queries in random order and records the number of misses.

8.2 Query speed/space tradeoffs in count queries

The VLBT variants supporting *count* operations improve query time over state-of-the-art run-length BWTs and compressed suffix arrays, while remaining competitive in space. Figure 6 summarizes the resulting space–time tradeoffs: panel (A) compares BWT-only structures, and panel (B) compares full compressed suffix arrays. Across datasets, the main outlier in speed is the move data structure, which is faster but substantially larger.

8.2.1 Run-length BWTs. The *vlbt-bwt* instances are between 1.15 and 2.3 times faster than *fbb*, while typically being between 1.06 and 4.6 times smaller. The size gap is particularly pronounced on COVID, where *vlbt-bwt* is 2.88–4.60

⁸<https://uud.ncbi.nlm.nih.gov/home/genomes>

⁹<https://github.com/torvalds/linux>

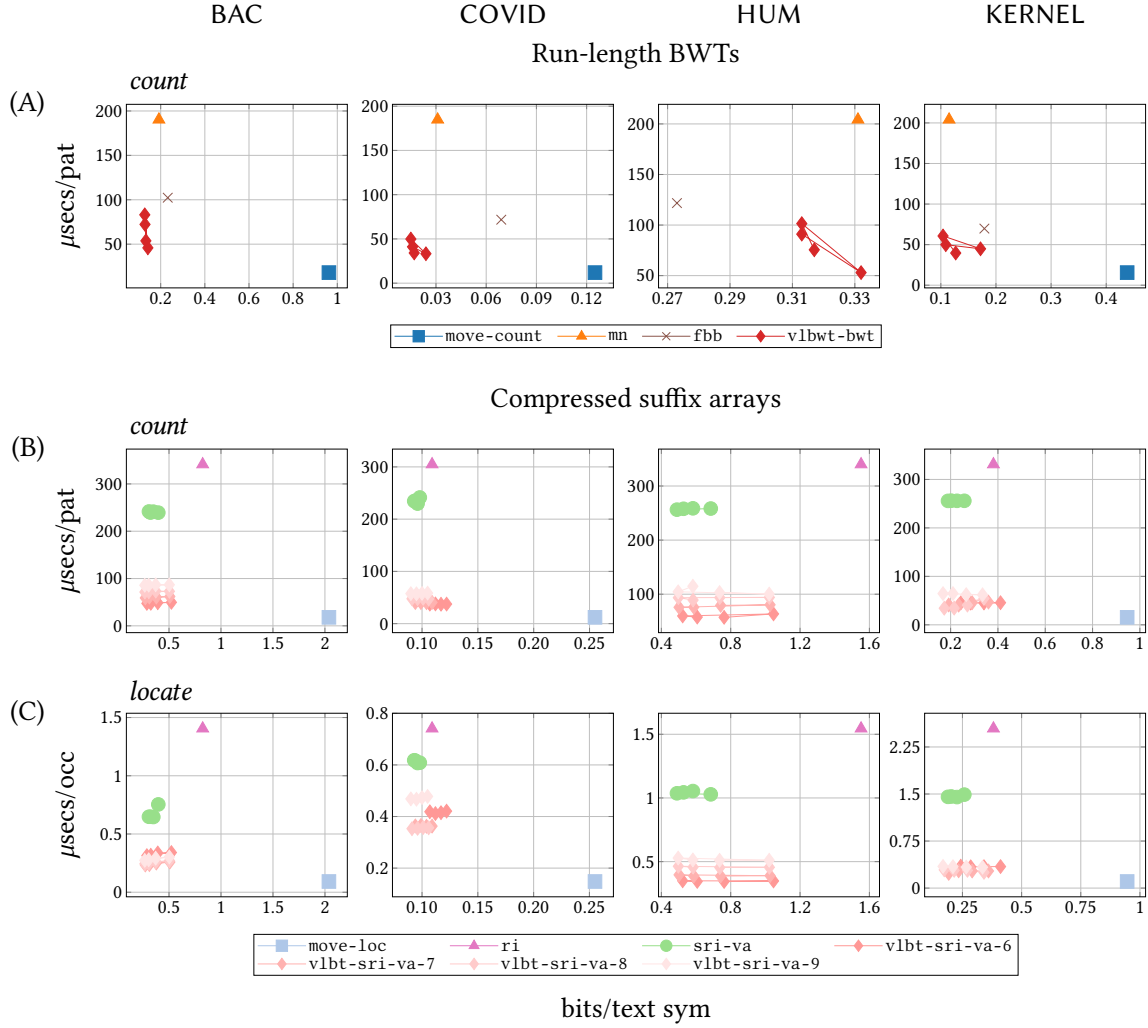


Fig. 6. Query speed/space tradeoffs. The points in each vlbwt-bwt are different block sizes ℓ , and the points in each vlbtsri-va-x are subsampling values s .

times smaller. This is consistent with the VLB-tree adapting its block boundaries to local run density, whereas fbb uses fixed-size blocks.

On the other hand, fbb achieves slightly better space usage on HUM, being 12.77%–17.77% smaller than vlbwt-bwt. This indicates that, for this dataset, fixed-block boosting can compress some locally dense regions slightly more effectively than our run-length encoding within leaves.

When compared to mn, vlbwt-bwt outperforms it in both space and time, achieving speedups of 2.01–5.55 while reducing space by up to a factor of 2.07.

Among the competing approaches, `move-count` offers a clear speed–space tradeoff: it is 2.56–4.54 times faster than `vlbt-bwt` but requires 2.55–8.33 times more space. Conversely, `vlbt-bwt` targets the opposite regime, prioritizing compactness while still improving over `mn` and `fbb` in query time.

8.2.2 Compressed suffix arrays. For `count` queries on compressed suffix arrays, `vlbt-sri-va` consistently improves over both `ri` and `sri-va` in query time. In terms of space, `vlbt-sri-va` and `sri-va` are broadly comparable when using equal subsampling settings, while `move-loc` remains the fastest option at the expense of substantially larger space consumption (Figure 6B).

Specifically, `move-loc` is typically 2.63–4.76 times faster than `vlbt-sri-va`, but also 2.23–5.63 times larger. The gap with `ri` is even more pronounced: `ri` is 3.22–8.14 times slower and up to 2.28 times larger than `vlbt-sri-va`.

Finally, when comparing *sr*-index variants across subsampling values s , `sri-va` is 2.37–6.81 times slower, while using comparable space. Depending on the chosen block size ℓ for `vlbt-sri-va`, `sri-va` can be almost equal in size or slightly larger, but the differences are modest compared to the consistent query-time gap. Overall, these results match our design goal: we preserve the components of the *sr*-index while reorganizing them to improve locality and reduce per-step overhead.

8.3 Query speed/space tradeoffs in `locate` queries

The `locate` results follow the same qualitative pattern across datasets (Figure 6C). Our `vlbt-sri-va` variants improve query time over `ri` and `sri-va` while remaining close to the space usage of subsampled indexes. Compared to `move-loc`, the results again highlight a clear space–time tradeoff: `move-loc` is faster, but substantially larger.

Overall, our `vlbt-sri-va` variants are between 1.57 and 9.64 times faster than `ri`, while requiring up to 2.28 times less space. The smallest improvement is observed on the COVID dataset, where our method achieves approximately a twofold speedup while using comparable space. This behavior is expected given the high repetitiveness of this dataset. Conversely, the largest space difference (2.28 factor) occurred in BAC, where sequence redundancy occurs within the same bacterial species, but not across species.

Compared to `sri-va`, the average speedups of our method range from 1.3 to 5.38, which is still considerable, but smaller than the gains in `count` queries when comparing the same data structures (2.37–6.36). A possible explanation is that, although a single operation $\phi^{-1}(SA[j])$ is more cache-friendly than its counterpart in `sri-va`, decoding consecutive values in $SA[sp_1 + 1..ep_1]$ remains cache inefficient in both cases.

The `move-loc` tool remains faster than our `vlbt-sri-va` variants, achieving speedups of 2.38 to 3.57 on average. However, this performance comes at a substantial space cost, as `move-loc` requires between 2.23 and 5.63 times more space. This difference is particularly pronounced for the BAC dataset, where the space overhead reaches a factor of 5.34–5.63. In contrast, the gap is smaller for COVID, with a factor of 2.23–2.62. These results are consistent with the observation that BWT-based approaches scale poorly in the presence of edits, as in BAC. While subsampling mitigates space growth, our adaptive encoding effectively improves query speed without incurring comparable space overhead.

8.4 Cache efficiency

Cache-miss measurements support the main explanation for the speedups observed above (Figure 7). Across datasets, our VLBT variants incur fewer L1 data-cache misses per query symbol than `fbb`, `mn`, `ri`, and `sri-va`, which is consistent with the corresponding reductions in query time (Figure 6). This indicates that memory locality is a primary driver of the observed performance differences.

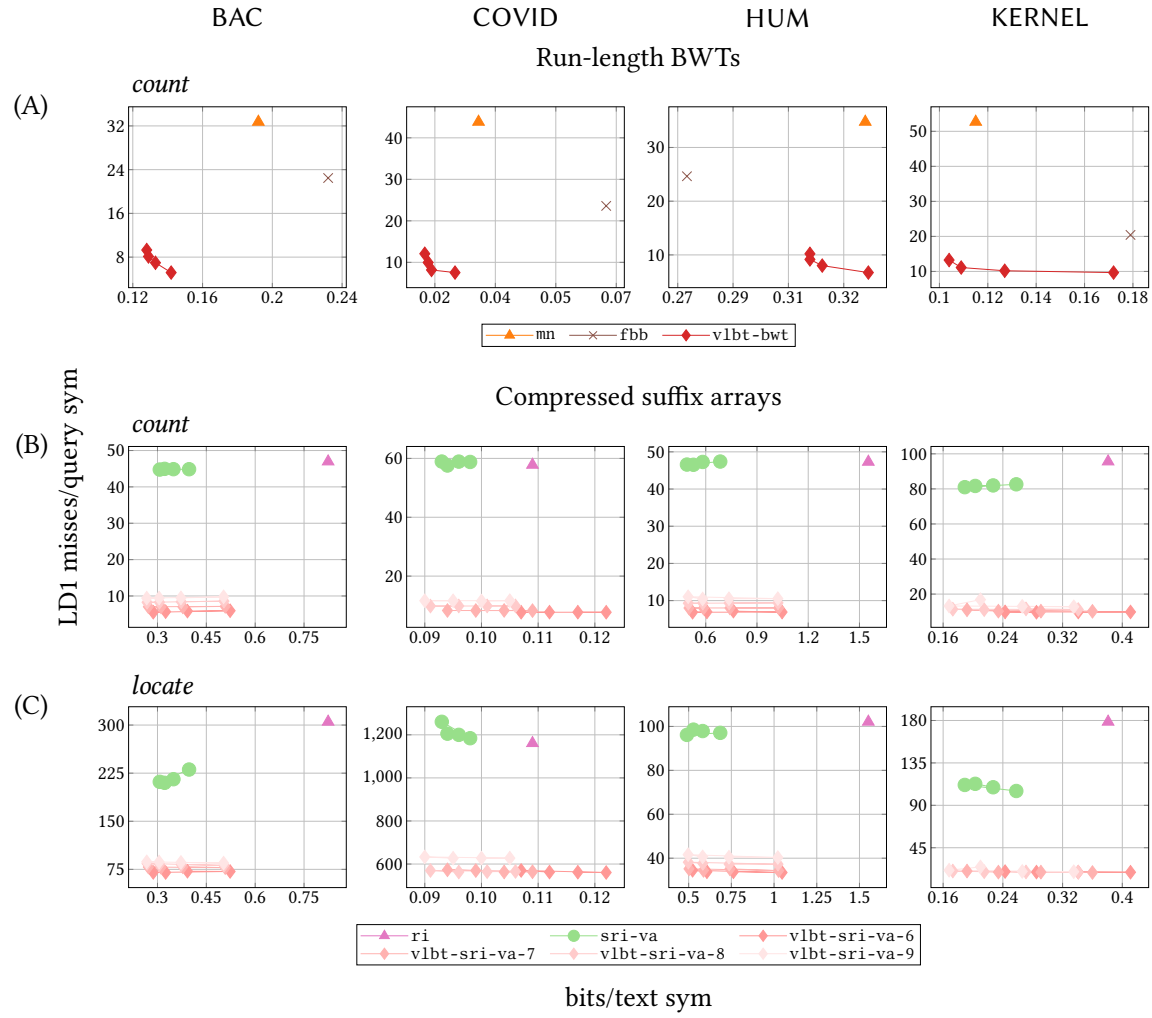


Fig. 7. L1 data cache misses/space tradeoffs.

For *count* queries on run-length BWTs, fbb incurs 1.54–4.35 times more misses than vlb-bwt, while mn incurs 3.41–6.33 times more misses. For compressed suffix arrays, the gap is larger: ri and sri-va trigger 4.51–9.84 and 4.48–8.46 times more misses on average, respectively.

For *locate* queries, ri triggers 1.85–9.34 times more cache misses than vlbtsri-va, while sri-va incurs 1.93–5.7 times more misses.

8.5 Effect of block size and subsampling

In vlb-bwt, increasing the block size from $\ell = 4^6$ to $\ell = 4^9$ reduces space usage by 5.72%–39.53%, depending on the dataset. The largest reduction (39.53%) occurs in COVID, which is consistent with larger alphabets increasing the fixed per-block overhead (e.g., alphabet-related metadata), so using fewer blocks yields larger savings. The smallest reduction

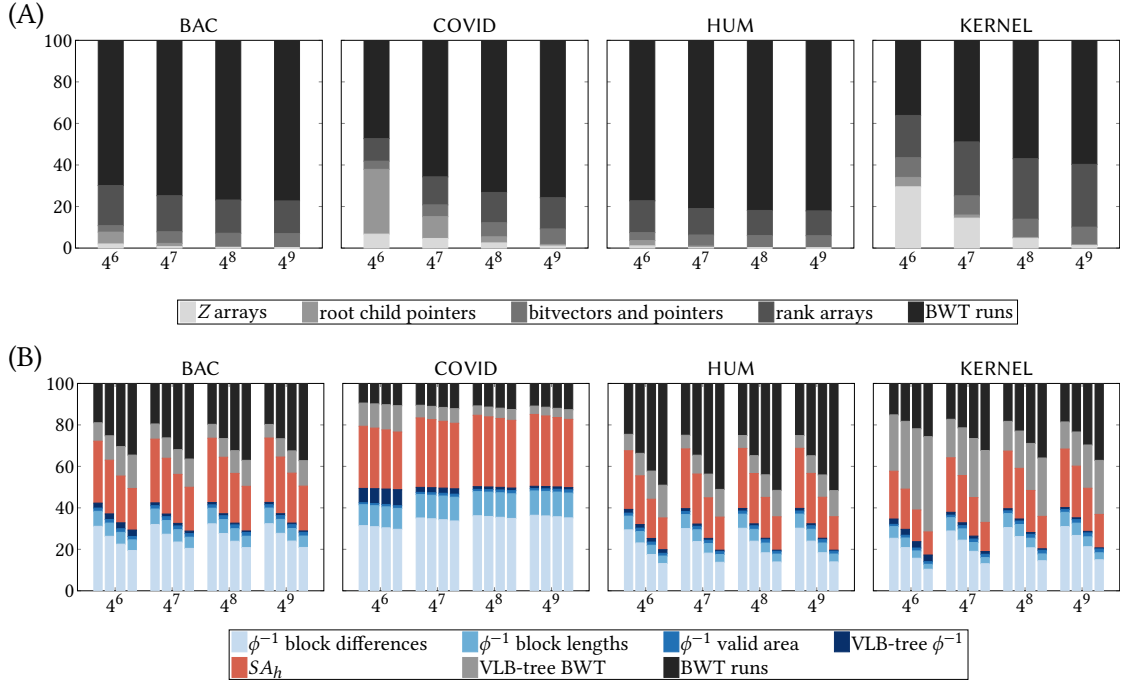


Fig. 8. Space breakdown in (A) `vlbt-bwt` and (B) `vlbt-sri-va`. The x-axis is the block size, and different bars in the same block size represent different subsampling values.

(5.72%) occurs in HUM, where the alphabet is small and the space is dominated by the encoded run structure rather than per-block metadata.

For `vlbt-sri-va`, changing ℓ has the same qualitative effect, and subsampling provides an additional (often larger) lever. The largest subsampling-driven reduction occurs in HUM: increasing s from 4 to 32 reduces the index size by approximately 51%.

8.6 Breakdown of space usage

In `vlbt-bwt`, the encoded BWT runs account for the largest fraction of the total space (36%–82%). As ℓ increases, this fraction grows because per-block satellite data is amortized across fewer larger blocks. Alphabet-related metadata can also be visible in the breakdown: for KERNEL, the root-level routing arrays Z (Section 3.4) reach up to 29% of the total space at $\ell = 4^6$. This overhead is reduced by the sampling technique of Section 5 and by using larger block sizes (Figure 8A).

In `vlbt-sri-va`, suffix-array samples (stored across SA_h and the VLB-tree for ϕ^{-1}) dominate the space budget, contributing between 21% and 71.09% of the total. Increasing the subsampling parameter s reduces this component by 3.02%–29.18% when moving from $s = 4$ to $s = 32$ (smallest reduction in COVID with $\ell = 4^9$; largest reduction in HUM with $\ell = 4^6$). The VLB-tree overhead (BWT and ϕ^{-1} trees plus validity metadata) is typically a smaller fraction (6.27%–21.72%), except in KERNEL where it reaches 50% (Figure 8B).

9 Conclusion

We presented the VLB-tree framework, an adaptive, cache-friendly encoding for BWT-based compressed suffix arrays. Across datasets, our structures improve query time over state-of-the-art r -index-based baselines while remaining competitive in space with the fast subsampled variant. The move data structure remains faster, but at a substantial space cost, highlighting a practical speed–space tradeoff.

Two directions appear particularly important for further practical progress. First, improving locality for ϕ^{-1} decoding remains challenging: consecutive values in $SA[sp_1..ep_1]$ are not necessarily recovered from contiguous areas of the ϕ^{-1} representation, which can limit *locate* performance. Second, scalable construction is still a bottleneck for terabyte-scale deployments. While recent work has improved BWT construction from compressed text [8, 24], comparable techniques for obtaining suffix-array samples at scale remain limited.

From a theoretical point of view, an open challenge is to derive space bounds that reflect the adaptivity of our method. In particular, worst-case guarantees for the VLB-tree of the BWT expressed only in terms of r , ℓ , and σ may fail to capture the main advantage of the approach: both ℓ and the satellite data adjust to local sequence content. Likewise, although the Z arrays near the top of the tree introduce an apparent σ -factor overhead, in practice this cost is moderated by our sampling strategy. A probabilistic analysis of the expected block structure would likely yield bounds that better match observed behavior.

References

- [1] Omar Y Ahmed, Massimiliano Rossi, Travis Gagie, Christina Boucher, and Ben Langmead. 2023. SPUMONI 2: improved classification using a pangenome index of minimizer digests. *Genome Biology* 24, 1 (2023), 122.
- [2] Nico Bertram, Johannes Fischer, and Lukas Nalbach. 2024. Move- r : Optimizing the r -index. In *Proc. 22nd International Symposium on Experimental Algorithms (SEA)*. Schloss Dagstuhl – Leibniz-Zentrum für Informatik, Dagstuhl, Germany, 1.
- [3] Christina Boucher, Travis Gagie, Alan Kuhnle, Ben Langmead, Giovanni Manzini, and Taher Mun. 2019. Prefix-free parsing for building big BWTs. *Algorithms for Molecular Biology* 14, 1 (2019), 13.
- [4] Christina Boucher, Travis Gagie, I. Tomohiro, Dominik Köppl, Ben Langmead, Giovanni Manzini, Gonzalo Navarro, Alejandro Pacheco, and Massimiliano Rossi. 2021. PHONI: Streamed Matching Statistics with Multi-Genome References. In *Proc. 31st Data Compression Conference (DCC)*. IEEE Computer Society, USA, 193–202.
- [5] Michael Burrows and David Wheeler. 1994. *A block sorting lossless data compression algorithm*. Technical Report 124. Digital Equipment Corporation.
- [6] Dustin Cobas, Travis Gagie, and Gonzalo Navarro. 2025. Fast and Small Subsampled R-indexes. *ACM Transactions on Algorithms* 22, 1 (2025), 29.
- [7] Diego Díaz-Domínguez, Saska Dónges, Simon J Puglisi, and Leena Salmena. 2023. Simple runs-bounded FM-index designs are fast. In *Proc. 21st International Symposium on Experimental Algorithms (SEA)*. Schloss Dagstuhl – Leibniz-Zentrum für Informatik, Dagstuhl, Germany, 7.
- [8] Diego Díaz-Domínguez and Gonzalo Navarro. 2023. Efficient construction of the BWT for repetitive text using string compression. *Information and Computation* 294 (2023), 105088.
- [9] Patrick Dinklage, Johannes Fischer, Lukas Nalbach, and Jan Zumbrink. 2025. RLZ- r and LZ-End- r : Enhancing Move- r . In *Proc. 32nd International Symposium on String Processing and Information Retrieval (SPIRE)*. Springer Nature Switzerland, Cham, 64–78.
- [10] Parsa Eskandar, Benedict Paten, and Jouni Sirén. 2025. Lossless Pangenome Indexing Using Tag Arrays. In *Proc. 25th International Conference on Algorithms for Bioinformatics (WABI 2025)*, Vol. 344. Schloss Dagstuhl – Leibniz-Zentrum für Informatik, Dagstuhl, Germany, 8.
- [11] Paolo Ferragina and Giovanni Manzini. 2005. Indexing compressed text. *J. ACM* 52, 4 (2005), 552–581.
- [12] Travis Gagie, Gonzalo Navarro, and Nicola Prezza. 2020. Fully Functional Suffix Trees and Optimal Text Searching in BWT-Runs Bounded Space. *J. ACM* 67, 1 (2020), 2.
- [13] Sara Giuliani, Shunsuke Inenaga, Zsuzsanna Lipták, Giuseppe Romana, Marinella Sciortino, and Cristian Urbina. 2025. Bit catastrophes for the Burrows-Wheeler transform. *Theory of Computing Systems* 69, 2 (2025), 19.
- [14] Simon Gog, Timo Beller, Alistair Moffat, and Matthias Petri. 2014. From theory to practice: Plug and play with succinct data structures. In *Proc. 13th International Symposium on Experimental Algorithms (SEA)*. Springer International Publishing, Cham, 326–337.
- [15] Simon Gog, Juha Kärkkäinen, Dominik Kempa, Matthias Petri, and Simon J Puglisi. 2019. Fixed block compression boosting in FM-indexes: Theory and practice. *Algorithmica* 81, 4 (2019), 1370–1391.
- [16] Roberto Grossi, Ankur Gupta, and Jeffrey Scott Vitter. 2003. High-order entropy-compressed text indexes. In *Proc. 14th Annual ACM-SIAM Symposium on Discrete Algorithms (SODA)*. Society for Industrial and Applied Mathematics, USA, 841–850.

- [17] Martin Hunt, Leandro Lima, Daniel Anderson, George Bouras, Michael Hall, Jane Hawkey, Oliver Schwengers, Wei Shen, John A Lees, and Zamin Iqbal. 2024. AllTheBacteria—all bacterial genomes assembled, available, and searchable. (2024). BioRxiv.
- [18] Ben Langmead. 2010. Aligning short sequencing reads with Bowtie. *Current Protocols in Bioinformatics* 32, 1 (2010), 11.7.1–11.7.14.
- [19] Daniel Lemire and Leonid Boytsov. 2015. Decoding billions of integers per second through vectorization. *Software: Practice and Experience* 45, 1 (2015), 1–29.
- [20] Heng Li and Richard Durbin. 2010. Fast and accurate long-read alignment with Burrows–Wheeler transform. *Bioinformatics* 26, 5 (2010), 589–595.
- [21] Veli Mäkinen and Gonzalo Navarro. 2005. Succinct suffix arrays based on run-length encoding. In *Proc. 16th Annual Symposium on Combinatorial Pattern Matching (CPM)*. Springer Berlin, Heidelberg, 45–56.
- [22] Udi Manber and Gene Myers. 1993. Suffix arrays: a new method for on-line string searches. *SIAM J. Comput.* 22, 5 (1993), 935–948.
- [23] Takaaki Nishimoto and Yasuo Tabei. 2021. Optimal-Time Queries on BWT-Runs Compressed Indexes. In *Proc. 48th International Colloquium on Automata, Languages, and Programming (ICALP)*, Vol. 198. Schloss Dagstuhl – Leibniz-Zentrum für Informatik, Dagstuhl, Germany, 101:1–101:15.
- [24] Jannik Olbrich. 2025. Fast and Memory-Efficient BWT Construction of Repetitive Texts Using Lyndon Grammars. In *Proc. 33rd Annual European Symposium on Algorithms (ESA)*, Vol. 351. Schloss Dagstuhl – Leibniz-Zentrum für Informatik, Dagstuhl, Germany, 60:1–60:19.
- [25] Massimiliano Rossi, Marco Oliva, Ben Langmead, Travis Gagie, and Christina Boucher. 2022. MONI: a pangenomic index for finding maximal exact matches. *Journal of Computational Biology* 29, 2 (2022), 169–187.
- [26] Kunihiko Sadakane. 2003. New text indexing functionalities of the compressed suffix arrays. *Journal of Algorithms* 48, 2 (2003), 294–313.
- [27] Li Song and Ben Langmead. 2024. Centrifuger: lossless compression of microbial genomes for efficient and accurate metagenomic sequence classification. *Genome biology* 25, 1 (2024), 106.
- [28] Ting Wang, Lucinda Antonacci-Fulton, Kerstin Howe, Heather A Lawson, Julian K Lucas, Adam M Phillippy, Alice B Popejoy, Mobin Asri, Caryn Carson, Mark JP Chaisson, et al. 2022. The Human Pangenome Project: a global resource to map genomic diversity. *Nature* 604, 7906 (2022), 437–446.
- [29] Peter Weiner. 1973. Linear pattern matching algorithms. In *Proc. 14th Annual Symposium on Switching and Automata Theory (SWAT)*. IEEE Computer Society, USA, 1–11.
- [30] Mohsen Zakeri, Nathaniel K. Brown, Omar Y. Ahmed, Travis Gagie, and Ben Langmead. 2024. Movi: a fast and cache-efficient full-text pangenome index. *Iscience* 27, 12 (2024), 111464.